

# Quantification of Adsorbed Flotation Reagents

Dominique Lascelles

*A thesis submitted to the Office of Graduate Studies and  
Research in partial fulfillment of the requirements for the  
degree of Master of Engineering*

Department of Mining, Metals and Materials Engineering  
McGill University  
Montreal, Canada

© Dominique Lascelles

February 2004



Library and  
Archives Canada

Bibliothèque et  
Archives Canada

Published Heritage  
Branch

Direction du  
Patrimoine de l'édition

395 Wellington Street  
Ottawa ON K1A 0N4  
Canada

395, rue Wellington  
Ottawa ON K1A 0N4  
Canada

*Your file* *Votre référence*

*ISBN: 0-612-98541-5*

*Our file* *Notre référence*

*ISBN: 0-612-98541-5*

#### NOTICE:

The author has granted a non-exclusive license allowing Library and Archives Canada to reproduce, publish, archive, preserve, conserve, communicate to the public by telecommunication or on the Internet, loan, distribute and sell theses worldwide, for commercial or non-commercial purposes, in microform, paper, electronic and/or any other formats.

The author retains copyright ownership and moral rights in this thesis. Neither the thesis nor substantial extracts from it may be printed or otherwise reproduced without the author's permission.

#### AVIS:

L'auteur a accordé une licence non exclusive permettant à la Bibliothèque et Archives Canada de reproduire, publier, archiver, sauvegarder, conserver, transmettre au public par télécommunication ou par l'Internet, prêter, distribuer et vendre des thèses partout dans le monde, à des fins commerciales ou autres, sur support microforme, papier, électronique et/ou autres formats.

L'auteur conserve la propriété du droit d'auteur et des droits moraux qui protègent cette thèse. Ni la thèse ni des extraits substantiels de celle-ci ne doivent être imprimés ou autrement reproduits sans son autorisation.

---

In compliance with the Canadian Privacy Act some supporting forms may have been removed from this thesis.

Conformément à la loi canadienne sur la protection de la vie privée, quelques formulaires secondaires ont été enlevés de cette thèse.

While these forms may be included in the document page count, their removal does not represent any loss of content from the thesis.

Bien que ces formulaires aient inclus dans la pagination, il n'y aura aucun contenu manquant.

  
**Canada**

*To Justin for the long train rides we  
have shared...*

*To David for his support and  
patience...soon it will be your turn.*

# Abstract

Collector interaction with mineral surfaces has long been studied. Little work has been done, however, on directly quantifying reagent adsorption, certainly under industrial process conditions. The use of a novel surface analysis technique, Headspace Analysis Gas-phase Infrared Spectroscopy (HAGIS), is suggested for quantification of adsorbed reagents in mineral processing.

As a first exercise, a test system of xanthate adsorption onto lead sulphide minerals was studied. A survey of possible calibration standards (pure xanthate, a synthetic lead-xanthate, galena (PbS) and a lead sulphide ore conditioned with xanthate) resulted in linear curves for all four cases. The quantification of isopropyl xanthate adsorption onto batch flotation products (concentrate and tail) was used to determine that ore standards gave the most accurate results.

The technique was also tested for quantification of adsorbed amines. Two collectors, dodecylamine and diphenylguanidine, and a depressant, triethylenetetramine, were studied. A common calibration curve was prepared using diphenylguanidine adsorbed on Inco matte. Results show that the HAGIS technique can easily be used to quantify adsorbed amines.

It is concluded that the HAGIS technique is a powerful new tool for the quantitative determination of adsorbed reagents. The xanthate study showed the use of ores as standards produces the best calibration. The amine study introduced the possibility of analyzing reagent mixtures.

# Résumé

L'interaction de réactifs avec la surface des minerais est source de plusieurs études depuis nombreuses années. Malgré ceci, peu d'attention est présentement dédiée à la quantification de l'adsorption des réactifs, surtout sous conditions communes à l'industrie. Ici, une nouvelle technique d'analyse des réactifs à la surface, l'analyse en phase gazeuse de l'espace de tête par spectroscopie infrarouge (HAGIS) est suggérée pour la quantification des réactifs adsorbés en procédés minéralurgiques.

En premier lieu, un système xanthate – minerais à base de sulfure de plomb fut étudié. Un survol de quatre standards possible (xanthate pur, xanthate de plomb, galène (PbS) et un minerai à base de sulfure de plomb conditionné avec du xanthate) présenta des courbes linéaires dans les quatre cas. La quantification du niveau d'adsorption d'un isopropyl xanthate à la surface de produits d'un essai de flottation en laboratoire (concentré et rejet) démontra que le minerai donne la courbe standard la plus exacte.

La technique fut aussi utilisée pour la quantification des aminés. Deux collecteurs, la dodécylamine et la diphénylguanidine, et un dépresseur, la triéthylènetetramine, furent étudiés. Une courbe de calibration commune fut préparée avec le système diphénylguanidine / matte Inco. Les résultats démontrent que la technique HAGIS peut être utilisée pour la quantification de réactifs ayant un groupe aminé.

En conclusion, il est évident que la technique HAGIS s'avère outil puissant pour la quantification de l'adsorption des réactifs. L'étude sur le xanthate démontre qu'une meilleure calibration est obtenue lorsque le minerai est utilisé en tant que standard. L'étude sur les aminés suggère qu'il soit possible d'utiliser la technique HAGIS pour la quantification simultanée d'un mélange de réactifs.

# Acknowledgements

Foremost, thanks go to Dr. J.A. Finch, FRSC, whose knowledge and capacity to take in massive quantities of information has made this work into a wonderful adventure.

Thanks must also go to Dr. Caroline Sui, for her friendship and trust that I would eventually find my way. Dr. S. Ramachandra Rao is acknowledged for his wealth of knowledge in chemistry and exciting suggestions. I would also like to thank Dr. Stéphanie Gélinas for being a friend and a sounding board for problems and ideas.

To all members of the Finch research group old and new, thanks for being there in work and procrastination.

I would also like to acknowledge financial support of the Natural Sciences and Engineering Research Council of Canada (NSERC) under the NSERC Collaborative Research and Development program sponsored by Inco, Falconbridge, Noranda, Teck Cominco, COREM and SGS Lakefield Research; and Brunswick Mine and Inco Limited for provision of samples.

I will forever be grateful to David and our son, Justin, for their understanding and patience. It has been a great exercise in teamwork.

# Contribution of Authors

This thesis was prepared in accordance with article C of the Guidelines Concerning Thesis Preparation of McGill University. The following are manuscripts written by the author that were used in preparation of this thesis. Manuscripts 1 and 2 make up Chapters 5 and 6, respectively.

1. **Dominique Lascelles and James A. Finch**, “Quantification of Adsorbed Reagents: Xanthate”, submitted to *Minerals Engineering*.
2. **Dominique Lascelles and James A. Finch**, “Quantification of Adsorbed Reagents: Amines”, to be submitted to *Minerals Engineering*.

Dr. James A. Finch is included as co-author in his capacity as research supervisor. Beyond his contributions, the author performed all of the work presented in this dissertation.

# Table of Contents

Abstract .....	i
Résumé.....	ii
Acknowledgements.....	iii
Contribution of Authors.....	iv
Table of Contents.....	v
List of Tables .....	viii
List of Figures .....	ix
1 Introduction .....	1
1.1 Mineral processing reagents .....	1
1.2 Detection of adsorbed reagents.....	3
1.3 Quantitative Analysis.....	4
1.4 Objectives .....	4
1.5 Structure of the thesis.....	5
2 Literature Review .....	7
2.1 Need for quantification of adsorbed reagents .....	7
2.2 Methods for determination of adsorbed species .....	8
2.2.1 X-ray Photoelectron Spectroscopy (XPS) .....	9
2.2.2 X-ray Absorption Spectroscopy (XAS).....	10
2.2.3 Secondary Ion Mass Spectrometry (SIMS) .....	11
2.2.4 Time-of-Flight Laser Ionization Mass Spectrometry (ToF-LIMS) .	12
2.2.5 Infrared Spectroscopy .....	14
2.2.6 Raman Spectroscopy.....	19
2.2.7 UV-Visible Spectroscopy .....	21
2.2.8 Thermal Desorption Methods .....	22



2.3	Conclusions.....	25
3	Quantitative Spectroscopy.....	26
3.1	Beer's Law.....	26
3.2	Gas Phase Quantitative Spectroscopy.....	30
3.3	Analysis Methods.....	31
3.3.1	Single Analyte Analysis.....	32
3.3.2	Multiple Component Analysis.....	35
4	Experimental Techniques.....	38
4.1	Introduction.....	38
4.2	UV-Visible Spectroscopy.....	38
4.3	Liquid Chromatography – Mass Spectrometry.....	39
4.4	Fourier Transform Infrared Spectroscopy (FTIR).....	39
4.5	Headspace Analysis Gas-Phase Infrared Spectroscopy (HAGIS).....	40
4.6	Batch Flotation Tests.....	41
5	Quantification of Adsorbed Reagents: Xanthate.....	42
5.1	Abstract.....	42
5.2	Introduction.....	42
5.3	Procedure.....	44
5.3.1	Calibration.....	44
5.3.2	Analysis.....	45
5.3.3	Flotation.....	47
5.4	Results.....	47
5.4.1	Comparison of HAGIS spectra.....	47
5.4.2	Calibration.....	49
5.4.3	Effect of Heating Time and Temperature.....	52
5.5	Discussion.....	53
5.6	Conclusions.....	54
6	Quantification of Adsorbed Reagents: Amines.....	55
6.1	Abstract.....	55
6.2	Introduction.....	55
6.3	Experimental.....	58

6.3.1	Reagents .....	58
6.3.2	Diphenylguanidine Adsorption on Inco Matte .....	58
6.3.3	Triethylenetetramine Adsorption on Voisey's Bay Nickel Co. Ore .....	58
6.3.4	Dodecylamine Adsorption on Quartz .....	59
6.3.5	HAGIS .....	59
6.3.6	UV-Visible .....	59
6.4	Results .....	60
6.4.1	Identification of Peaks .....	60
6.4.2	Calibration Curve – DPG on Inco Matte .....	62
6.4.3	Mass Balance .....	63
6.5	Discussion .....	65
6.6	Conclusions .....	65
7	Conclusions .....	67
7.1	Protocol for the Quantification of Adsorbed Reagents using HAGIS ..	67
7.2	Future Work .....	69
	References .....	70

# List of Tables

Table 5-1 Xanthate decomposition peak positions and peak areas (% contribution to total for these four peaks).....	48
Table 5-2 Comparison of calibration procedures for the determination of IPX adsorption onto Brunswick Mine ore flotation products (reported as mg).....	51
Table 5-3 Xanthate adsorption levels (mg/g) on Brunswick Mine batch flotation products (Ore calibration).....	52
Table 6-1 Band Maxima in the Infrared Vapour Phase Spectra of Amines in the 1250 to 700 cm <sup>-1</sup> range. ....	61
Table 6-2 Mass balance for DPG adsorbed on Inco Matte.....	63
Table 6-3 Mass balance of TETA adsorbed on Voisey's Bay Nickel Co. ore. ....	64
Table 6-4 Dodecylamine adsorption on quartz. ....	64

# List of Figures

Figure 2-1 Absorption of x-ray photon and emission of photoelectron.....	9
Figure 2-2 Schematic of ToF-LIMS analysis instrumentation (Bolin et al.).....	13
Figure 2-3 Schematic of specular and diffuse reflectance (Baulsir and Tague). ...	16
Figure 2-4 Optical diagram of an ATR prism showing the amplitude decay of the evanescent wave (Cases and De Donato) where $E_0$ and $E$ are the amplitudes of the electric field at the ATR surface and in the sample respectively. ....	17
Figure 2-5 IR beam direction and polarization in ATR setup (Larsson et al.). ....	18
Figure 2-6 Schematic representation of surfactant orientation relative to order number (Singh et al.).....	19
Figure 2-7 Representation of heptylxanthate bridging coordination to a ZnS surface with resulting tilt angle of $37^\circ$ (Larsson et al.). ....	19
Figure 2-8 Raman scattering processes compared to infrared absorption (Kariis). ....	20
Figure 2-9 Photo of loaded HAGIS cell (Lascelles et al.). ....	24
Figure 3-1 Absorbance of photons by a sample (Smith). ....	27
Figure 4-1 Asymmetric stretching of a $\text{CO}_2$ molecule.....	40
Figure 4-2 HAGIS cell (open) showing filled sample boat and Teflon endcaps.....	41
Figure 5-1 HAGIS Peak integration scheme for xanthate. ....	46
Figure 5-2 HAGIS spectra for (a) NaIPX, (b) $\text{Pb}(\text{IPX})_2$ , (c) galena + IPX, and (d) Brunswick Mine ore + IPX. ....	48
Figure 5-3 HAGIS calibration curve for sodium isopropyl xanthate (NaIPX) (a) pure and (b) derived from $\text{Pb}(\text{IPX})_2$ . ....	49
Figure 5-4 HAGIS calibration curve for IPX adsorbed onto galena. (mg IPX determined by difference using UV/Vis analysis on solutions).....	50

Figure 5-5 HAGIS calibration curve for IPX adsorbed onto Brunswick Mine ore. Data points are a combination of changing IPX mass and sample mass. ....	50
Figure 5-6 Effect of heating time on COS peak area at two temperatures: 190°C and 250°C. ....	53
Figure 6-1 Schematic diagram for (a) dodecylamine, (b) diphenylguanidine and (c) triethylenetetramine. ....	57
Figure 6-2 HAGIS peak integration scheme for amines.....	60
Figure 6-3 HAGIS spectra for the desorption products of (a) dodecylamine on quartz, (b) triethylenetetramine on Voisey’s Bay Nickel Co. ore, (c) diphenylguanidine on Inco matte. ....	61
Figure 6-4 HAGIS calibration curve for DPG adsorbed onto Inco matte (mg DPG determined by difference using UV/Vis analysis on solutions).....	62
Figure 6-5 “Universal” HAGIS calibration curve for amines (derived from DPG on Inco matte). ....	63
Figure 7-1 HAGIS peak integration scheme.....	68

# List of Equations

$A = \epsilon l c$	Equation 1-1.....	4
$c_{\text{unknown}} = \frac{A}{\epsilon l}$	Equation 1-2.....	4
$\theta_c = \sin^{-1} \frac{n_2}{n_1}$	Equation 2-1.....	17
$D = \frac{A_s}{A_p}$	Equation 2-2.....	18
$S = 1.5 \cos^2 \gamma - 0.5$	Equation 2-3 .....	18
$-dI \propto I c dl$	Equation 3-1.....	28
$-dI = \epsilon I c dl$	Equation 3-2 .....	28
$-\frac{dI}{I} = \epsilon c dl$	Equation 3-3 .....	28
$\ln \frac{I_0}{I} = \epsilon c l$	Equation 3-4 .....	28
$\log \frac{I_0}{I} = \epsilon c l$	Equation 3-5 .....	28
$A = \log \frac{1}{T}$	Equation 3-6 .....	29
$T = 10^{\epsilon c L}$	Equation 3-7 .....	29
$c = \frac{P}{RT}$	Equation 3-8 .....	30
$c = \frac{A}{\epsilon l}$	Equation 3-9 .....	31
$A = \frac{P \epsilon l}{RT}$	Equation 3-10 .....	31

$R = \left( \frac{SSR}{SST} \right)^{\frac{1}{2}}$	Equation 3-11.....	33
$F = \frac{SSR (n - m - 1)}{SSE m}$	Equation 3-12.....	33
$A_1 = \varepsilon_{1a}lc_a + \varepsilon_{1b}lc_b + \varepsilon_{1c}lc_c$		
$A_2 = \varepsilon_{2a}lc_a + \varepsilon_{2b}lc_b + \varepsilon_{2c}lc_c$	Equation 3-13.....	35
$A_3 = \varepsilon_{3a}lc_a + \varepsilon_{3b}lc_b + \varepsilon_{3c}lc_c$		
$\begin{pmatrix} A_1 \\ A_2 \\ A_3 \end{pmatrix} = \begin{pmatrix} \varepsilon_{1a} & \varepsilon_{1b} & \varepsilon_{1c} \\ \varepsilon_{2a} & \varepsilon_{2b} & \varepsilon_{2c} \\ \varepsilon_{3a} & \varepsilon_{3b} & \varepsilon_{3c} \end{pmatrix} \begin{pmatrix} l \\ l \\ l \end{pmatrix} \begin{pmatrix} c_a \\ c_b \\ c_c \end{pmatrix}$	Equation 3-14.....	35
$A = ELC$		
$A = KC$	Equation 3-15.....	36
$K = AC^T(CC^T)^{-1}$	Equation 3-16.....	36
$C_{unk} = (K^TK)^{-1}K^TA_{unk}$	Equation 3-17.....	36
$C = PA$	Equation 3-18.....	36
$P = CA^T(AA^T)^{-1}$	Equation 3-19 .....	36

# 1 Introduction

## 1.1 Mineral processing reagents

Mineral processing involves the separation of the desired mineral (valuable) from the gangue (non-valuable). In flotation this is achieved by selective attachment to air bubbles, the resulting bubble/particle aggregate rising to form a froth. To attach to air bubbles, the mineral must have a hydrophobic (i.e., water repellent) surface. Because most naturally occurring minerals are hydrophilic (i.e., water attractant), organic reagents called collectors are used to make the surface hydrophobic.

Collectors are, for the most part, heteropolar organic reagents; i.e., comprise a non-polar (hydrophobic) hydrocarbon chain and a polar (hydrophilic) head group. In most cases, the hydrophilic part reacts with the mineral surface, the process leading to adsorption of the collector. This orientation leaves the hydrophobic part exposed to the water, rendering the mineral surface hydrophobic; i.e., the mineral becomes “floatable”.

In some cases, activators are used to promote interaction with collectors for minerals that otherwise show little response. The classic case is activation of sphalerite, a zinc sulphide, by copper ions. Here, the copper ions exchange with



## Chapter 1 – Introduction

---

zinc ions in upper layers of the lattice and make the sphalerite surface appear to be a copper sulphide with which the common sulphide mineral collector xanthate readily interacts<sup>1</sup>.

Reagents known as depressants act the opposite of activators, making a mineral not float that otherwise would. They can either render the surface hydrophilic or block collector adsorption. They can be organic (e.g., guar, starch, dextrin, carboxymethylcellulose (CMC)) or inorganic (e.g., lime, cyanide, sulphide, chromate, and ferrocyanate) substances.

One class of depressants removes activating species. These reagents may be used to reverse activation or, more commonly, prevent the inadvertent activation of a mineral by metal ion species released due to superficial oxidation from other minerals present in the pulp. The reagents may be termed deactivators or cleaning agents. One type of cleaning agent forms soluble coordination complexes with activating species such as copper and nickel ions<sup>2-4</sup>.

Frothers are used to prevent air bubble coalescence maintaining fine bubbles and resulting in high bubble surface area flux in the pulp and a stabilized froth on the surface. Generally, frothers have a hydroxyl end group with a hydrocarbon chain. This induces the frother to accumulate (adsorb) at the air-water interface (i.e., bubble surface). Leja and Schulman have suggested that frother molecules interpenetrate the adsorbed collector layer thus promoting particle/bubble adherence<sup>5</sup>.

Although collector interaction with mineral surfaces has long been studied, little work has been done to quantify directly the amount adsorbed, certainly in the industrial process. The advantage of knowing the quantity of adsorbed reagents is twofold: it may allow for proper accounting of reagents used in the process to satisfy environmental regulations, and it becomes a tool for better management of reagent consumption.

## Chapter 1 – Introduction

---

### 1.2 Detection of adsorbed reagents

The most common techniques for organic reagents are based on infrared and to a lesser extent Raman spectroscopy. These are widely used to identify surface species but are difficult to adapt to quantitative analysis, in part because most procedures required the use of concentrations 10-100 times higher than those used in ore flotation to obtain adsorption information<sup>6,7</sup>. There have been studies using thermal decomposition of adsorbed collector as part of the analytical procedure<sup>8,10</sup>. The methods give good reproducibility. There is some concern, however, that the techniques rely on carbon species analysis and it is known that carbon tends to be present as a contaminant at the particle surface (e.g., from CO<sub>2</sub> present in the air or in aqueous solution). The use of Time-of-Flight Secondary Ion Mass Spectrometry (ToF-SIMS) and Laser Ion Mass Spectrometry (ToF-LIMS) has shown very good characterization of individual particle coverage but a large number of particles need to be analyzed to obtain acceptable reproducibility, which is time consuming and costly<sup>6,11-13</sup>.

Infrared spectroscopy remains an attractive technique because it details the molecular structure of adsorbed reagents. Vreugdenhil et al. have reported the detection of xanthates at concentrations comparable to industrial use employing Headspace Gas-Phase Infrared Spectroscopy (HAGIS)<sup>7</sup>. By heating the mineral sample, the organic species are desorbed into the gas-phase, which is held in the space above the sample boat (headspace). The technique is convenient because the sample size can be increased to obtain higher concentrations of desorbed collector in the headspace (i.e., the detection limit for surface species is reduced accordingly). Thus far, quantification of adsorbed reagents has not been attempted with this technique. This is the subject of this thesis.

## Chapter 1 – Introduction

---

### 1.3 Quantitative Analysis

Although not common, it is possible to perform quantitative analysis using Infrared spectroscopy<sup>14,15</sup>. The basis is Beer's law which relates concentration (c) to absorbance (A) in the following form:

$$A = \epsilon l c \quad \text{Equation 1-1}$$

The absorbance, A, is related to the concentration, c, by the absorptivity,  $\epsilon$ , and the sample pathlength, l. Absorptivity is a property of the molecule and the wavenumber of the incident radiation. The units for absorptivity are (concentration x pathlength)<sup>-1</sup> and absorbance is therefore dimensionless. The absorbance may be measured as peak height, peak area, or a ratio of peaks from the FTIR spectrum.

Calibration using Beer's law is made by plotting the absorbance or the integrated peak area of standards at a specific wavenumber, versus concentration. If the plot is linear then Beer's law is obeyed and the straight line is the calibration curve. The slope of the calibration curve is therefore  $\epsilon \times l$  and the model becomes:

$$c_{\text{unknown}} = \frac{A}{\epsilon l} \quad \text{Equation 1-2}$$

The concentration of the unknown is obtained by dividing the absorbance value (peak height or peak area) by the slope of the calibration curve.

The theory of quantitative spectroscopy and Beer's law will be discussed further in Chapter 3.

### 1.4 Objectives

The general objective is to explore the use of the HAGIS technique for the detection and quantification of adsorbed reagents, collectors in particular, used in

## **Chapter 1 – Introduction**

---

mineral flotation. The hypothesis is that all organic reagents adsorbed on mineral surfaces can be analyzed using the technique.

To test, a mass balance will be performed for a system of galena and xanthate using Ultraviolet/Visible spectroscopy to determine indirectly the amount adsorbed by measuring residual xanthate in solution while the HAGIS technique determines adsorbed xanthate directly on concentrate and tails. Following, xanthate adsorption on batch flotation products will be attempted using the proposed procedure.

The versatility of the technique will be explored in identifying and quantifying chelating-type collectors. If successful, a protocol for the determination of adsorbed flotation reagents on industrial process samples will be proposed.

### **1.5 Structure of the thesis**

The thesis consists of seven chapters. Chapter one introduces mineral processing reagents and different methods of identifying and quantifying them. Chapter two reviews in more detail recent advances in quantifying adsorbed reagents. In chapter three, quantitative spectroscopy and the validity of using the HAGIS technique for quantitative analysis are detailed. The experimental setup and procedures are outlined in Chapter 4.

Chapters 5, and 6 are presented as manuscripts. Chapter 5, **Quantification of Adsorbed Flotation Reagents: Xanthate** by D. Lascelles, and J.A. Finch, shows the general potential of the HAGIS technique and demonstrates quantification of adsorbed xanthate. In this chapter, four standard calibration systems are tested. A protocol is advanced for quantitative analysis using the HAGIS technique.

In Chapter 6, **Quantification of Adsorbed Flotation Reagents: Amines** by D. Lascelles, and J.A. Finch, the capabilities of the HAGIS technique in determining

## **Chapter 1 – Introduction**

---

chelating-type collector (diphenylguanidine) and depressant (triethylenetetramine) adsorption is explored. The protocol determined in Chapter 5 is followed.

Finally, Chapter 7 presents conclusions that may be drawn from the work and further research possibilities are explored.

## **2 Literature Review**

### **2.1 Need for quantification of adsorbed reagents**

In mineral processing, the most common process for separation of valuable minerals from each other and from non-valuable gangue is selective flotation. Organic reagents called “collectors” are added to a slurry to make the desired mineral hydrophobic. Collectors are usually heteropolar, having hydrophilic and hydrophobic groups. They will typically adsorb at the mineral surface through the hydrophilic group, leaving the hydrophobic group oriented towards the water, making the surface hydrophobic and allowing the mineral particle to attach to air bubbles.

Proper accounting of flotation reagents would be a clear benefit in mineral processing. It would allow for better management of reagents, which will result in greater economic return both in terms of product quality and reduced reagent consumption. There is also an advantage to satisfy increasingly strict environmental regulations, by being able to do reagent “accounting”. Fundamentally, quantification and knowledge of the distribution of added reagents in the process will help increase understanding of the process. For example, an often-raised question is whether good selectivity is due to the adsorption of collector on the valuable mineral or of depressant on gangue. Surface coverage data may help interpret adsorption mechanisms. Moreover,

## **Chapter 2 – Literature Review**

---

some of the surface analysis techniques are capable of indicating how the reagent is adsorbed.

The focus of this work is to determine the amount of adsorbed reagents on mineral surfaces. The following review of recent literature outlines the techniques that have been and are currently being used for the determination of adsorbed reagents. The aim of the chapter is to prepare a list of available techniques and to evaluate them on the usefulness of the information they give and on their ability to give quantitative data.

### **2.2 Methods for determination of adsorbed species**

The current methods available for identifying and quantifying adsorbed species can be divided into three broad categories:

1. Direct analysis of surface molecules by: electron bombardment through x-ray photoelectron and absorption spectroscopy (XPS and XAS), time-of-flight – secondary ion mass spectrometry (ToF-SIMS), and laser ionization mass spectrometry (LIMS), or electromagnetic spectroscopy through surface enhanced raman and infrared spectroscopy (SERS and IR).
2. Indirect analysis by measurement of residual reagents in solution or through solvent extraction combined with ultraviolet-visible spectroscopy or infrared spectroscopy.
3. Thermal desorption/decomposition coupled with (i) combustion to CO<sub>2</sub> and analysis by infrared, (ii) differential thermal analysis, and (iii) gas-phase spectroscopy such as thermogravimetry combined with infrared (TG-FTIR) or headspace analysis gas-phase infrared spectroscopy (HAGIS).

## Chapter 2 – Literature Review

---

These techniques are discussed with reference to analysis of adsorbed reagents. Particular attention is given to the amenability of each technique to the quantification of adsorbed flotation reagents in the range observed in operations.

### 2.2.1 X-ray Photoelectron Spectroscopy (XPS)

In photoelectron spectroscopy the sample is illuminated with soft (1.5kV) x-rays (Al K $\alpha$  or Mg K $\alpha$ ) in an ultrahigh vacuum. The x-rays remove electrons from core levels within the atom (Figure 2-1). The energy of the photoelectrons emitted (binding energy) from an atom is characteristic of the element and dependent on the electronegativity of the atom. The presence of chemical bonds will cause binding energy shifts. These chemical shifts allow for the identification of elemental oxidation states and structural effects. Because photoelectrons are strongly attenuated when passing through the sample, the information obtained comes from the top 1-5 nm of the surface only.

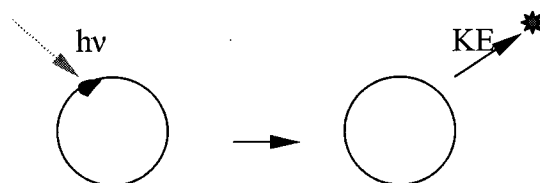


Figure 2-1 Absorption of x-ray photon and emission of photoelectron.

Many studies have focused on the surface of natural sulphide minerals. Buckley et al.<sup>16</sup> and Brienne et al.<sup>17</sup> studied the surface species of natural sphalerite under flotation related conditions but did not look at the possible identification of adsorbed collectors. Smart<sup>18</sup> has suggested that the sulphur S<sub>2p</sub> peak could help determine the mechanism of xanthate adsorption onto sulphide mineral surfaces. In studies of Cu-activated sphalerite conditioned with ethylxanthate, Lascelles et al.<sup>19</sup> reported a difference in the S<sub>2p</sub> peak after conditioning with xanthate. Petrovykh et al.<sup>20</sup> reported quantitative analysis of DNA immobilized on gold



## **Chapter 2 – Literature Review**

---

using the  $N_{1s}$ ,  $P_{2p}$ ,  $C_{1s}$ , and  $O_{1s}$  peaks. Allen et al.<sup>21</sup> used XPS to determine the adsorption of polyacrylamide onto kaolin, feldspar and quartz. Glass slides treated with varying concentrations of polyacrylamide showed a direct relationship between concentration and  $N_{1s}$  peak height suggesting the possibility of quantitative determination using this technique. The detection of collector molecules on mineral surfaces from operating flotation plants has also been reported with the XPS technique<sup>18,22</sup>.

Laajalehto et al.<sup>23</sup> used synchrotron radiation to improve surface sensitivity in the identification of surface species of submonolayer coverage. Synchrotron radiation provides a continuous energy distribution over a large energy region rather than a fixed excitation energy source as in conventional XPS. Szargan et al.<sup>24</sup> used SRXPS to determine the adsorbate species of 2-mercaptobenzothiazole (MBT) onto galena. Adsorption of 5-methyl-2-mercaptobenzoxazole (MMBO) onto chalcocite ( $Cu_2S$ ) has also been studied<sup>25</sup>.

### **2.2.2 X-ray Absorption Spectroscopy (XAS)**

Rather than emission, another possibility is the use of absorption with x-ray spectroscopy. Patrick et al.<sup>26</sup> used fluorescence reflection extended X-ray absorption fine structure (fluorescence REFLEXAFS) to observe the interaction of Cu with a sphalerite surface and the effect of xanthate addition. In REFLEXAFS, the x-ray is directed to hit the sample surface at a very low angle where the beam is reflected, rather than being absorbed. The penetration depth is usually less than 50 Å making this a surface sensitive technique. Patrick et al. reported that upon addition of xanthate, oxygen was displaced from the surface and a covellite-like ( $CuS$ ) species is formed. Use of this technique for quantitative analysis has not been reported.

## **Chapter 2 – Literature Review**

---

### **2.2.3 Secondary Ion Mass Spectrometry (SIMS)**

Upon sputtering of a solid sample with primary ions, a fraction of the particles emitted from the target is ionized. The SIMS technique analyzes these secondary ions with a mass spectrometer. Secondary ion emission provides information on the elemental, isotopic and molecular composition of the uppermost atomic layer (the top monolayer) of a solid surface. O'Dea et al.<sup>27</sup> have reported on the interaction of xanthate with galena using static SIMS. They observed nucleation of high xanthate concentration at lead oxide/hydroxide precipitate sites, suggesting that there is ion exchange between the xanthate and the hydroxide followed by oxidation to dixanthogen and diffusion across the surface. Nagaraj and Brinen<sup>28,29</sup>, have reported extensive studies on SIMS identification of collector adsorption on single mineral specimens.

Adsorbed dodecylbenzenesulfonate (DBS) concentrations on unhydrated portland cement has been quantitatively determined by plotting the fragment ratios  $\text{O}^-/\text{C}^+/\text{Ca}^+$  and  $\text{SO}_3^-/\text{O}^-$  (surfactant/cement matrix) against surfactant concentration<sup>30</sup>. A linear relationship was obtained up to monolayer coverage.

Time of Flight Secondary Ion Mass Spectrometry (ToF-SIMS) varies from static SIMS in that the ejected ions are accelerated into the analyzer with a common energy but achieve different velocities due to particle mass. The variation in velocities is used to determine the mass of the secondary ions by observing their travel time through the analyzer. This method permits the investigation of the bulk composition or a depth distribution of trace elements. The technique has proved useful in identifying impurities that may affect mineral flotation performance<sup>31</sup>. Surface concentrations of potassium isobutyl xanthate and sodium diisobutyl dithiophosphate were not distinguishable when studied on particles of different sizes of galena in flotation concentrate and tails. A statistical difference was observed, however, when the particles compared were of the same size.

## **Chapter 2 – Literature Review**

---

ToF-SIMS has also been used for chemical mapping. In the case of protein adsorption onto stainless steel, preferred adsorption sites were determined as impure salt residue precipitated at the surface<sup>32</sup>. Boulton et al.<sup>6</sup> have reported patchy collector adsorption on pure mineral mixtures (20g Sp and 80g Py; collector dosage 100-200g/t) with clear differences in adsorption of hydrophobic species between concentrates and tails. Chryssoulis and coworkers<sup>33</sup> have imaged the non-uniform adsorption of a mixture of amyldithiophosphate and amyloxanthate on concentrate and tailings samples from three Canadian concentrators (Kidd Creek, Matagami, and Brunswick). Although the technique can determine relative concentrations on particles of the same mineral (and of the same size range), it cannot, at this time, quantify collector adsorption.

Some challenges in the quantification of adsorbed organic species are due to the role of the chemistry of the substrate (matrix effect). The ToF-SIMS spectrum of certain compounds can change depending on the environment; e.g. the secondary ion yield pattern varies depending on chemical bonding to the matrix<sup>31,34</sup>. An international round-robin experiment has been conducted in an attempt to reduce these matrix effects<sup>35</sup>. At present, ToF-SIMS is better suited to quantify differences between two products (e.g., comparing collector concentration on Sp grains from concentrate and tail samples) than absolute quantities.

### **2.2.4 Time-of-Flight Laser Ionization Mass Spectrometry (ToF-LIMS)**

In ToF-LIMS, a laser pulse removes material from the surface (ablation) and creates a microplasma that ionizes some of the sample constituents. The laser pulse both vaporizes and ionizes the sample. The laser beam, usually generated by a Nd:YAG (Neodymium doped Yttrium Aluminum Garnet) laser source set at 266 nm, is focused to a spot of 2-4  $\mu\text{m}$  diameter. Figure 2-2 shows a typical ToF-LIMS analysis setup. In positive mode (Figure 2-2a), a second laser ionizes the ablated neutral particles. The ionized particles are accelerated into a time of flight mass spectrometer by applying a negative potential to the sample holder. Bolin et

## Chapter 2 – Literature Review

al.<sup>11</sup> have used the technique to study the effect of “pre-activation” of pyrite in a copper-lead ore. They reported a large concentration of Cu and Pb ions (activators) on pyrite misreporting to the copper-lead concentrate along with significantly lower levels of Ca and Fe ions (depressants) relative to the levels found on the pyrite in the tails. Martin et al.<sup>36</sup> have also used positive ionization in the characterization of mine tailings. In negative mode (Figure 2-2b), only one laser source is used and the polarity of the electrostatic field is reversed. Negative ionization permits the analysis of anionic constituents such as many collector molecules.

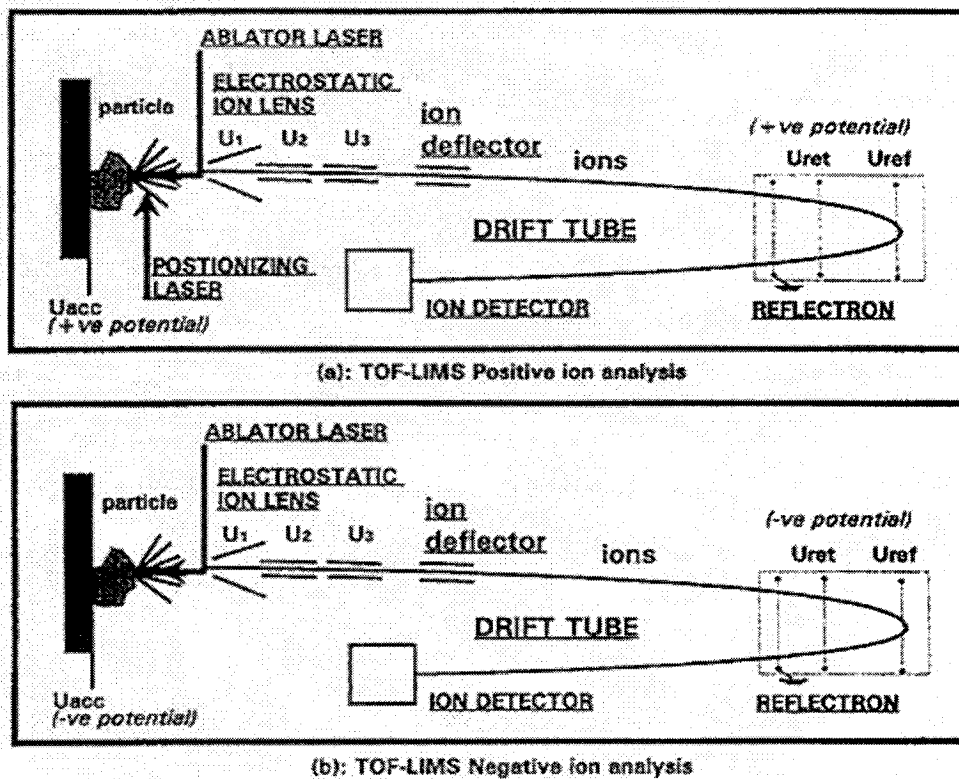


Figure 2-2 Schematic of ToF-LIMS analysis instrumentation (Bolin et al.)<sup>11</sup>.

ToF-LIMS is well established as a qualitative and semi-quantitative analysis technique. There are several factors that make accurate quantitative analysis problematic; energy deposition in the sample, ion formation, extraction and transmission of ions, and the detection system are the major factors affecting

## Chapter 2 – Literature Review

---

signal intensity. Dimov and Chryssoulis<sup>37</sup> have suggested a series of steps to minimize the sources of variability. They report that the use of separate laser ablation and ionization steps has the potential to provide quantitative elemental analysis of mineral surfaces in the positive mode.

Shi et al.<sup>38</sup> used vacuum ultraviolet (VUV) laser excitation ( $< 200$  nm) for qualitative and quantitative analysis of xanthate esters. The esterification of xanthates results in products that are more volatile than xanthates and therefore easier to analyze by VUV radiation. Preliminary results show detection limits in the subfemtomole ( $\sim 4.1 \times 10^{-14}$  mol) region.

### 2.2.5 Infrared Spectroscopy

There are three types of motion that a molecule may undergo, translational motion (i.e., spatial movement), rotational motion (i.e., rotation about an internal axis), and vibrational motion (i.e., stretching and bending of bonds). Vibrational motions occur at frequencies of about  $10^{14}$  s<sup>-1</sup>, which is equivalent to a wavelength of  $3 \times 10^{-4}$  cm (3000 nm). Therefore, the energy required for vibrational frequencies lies in the infrared region of the spectrum. In IR spectroscopy, the vibrational frequencies are observed by determining the amount of light absorbed from an infrared light beam transmitted through the sample. The absorption intensity is plotted against the frequencies at which these molecules vibrate in order to determine the specific bond that is vibrating.

Conventional IR techniques include encapsulating a sample in a KBr pellet or a nujol mull but these cannot be applied to aqueous environments because the O-H absorption of water is too strong. The infrared analysis of collector adsorption onto sulphide mineral surfaces has been documented using the KBr technique<sup>39,40</sup>. The adsorbed species were extracted with a common solvent, mixed with a known amount of KBr, the solvent evaporated, and a pellet formed. Miettinen et al.<sup>40</sup> have reported the detection of as little as 20g/t collector. Direct transmittance

## **Chapter 2 – Literature Review**

---

infrared studies can also be achieved when the mineral studied shows good transmittance. In the case of sphalerite, slices 0.5 to 1 mm in thickness result in pale yellow plates having transmittance values of about 50% in the 1300  $\text{cm}^{-1}$  to 900  $\text{cm}^{-1}$  region<sup>41</sup> (where C-S and C-O vibrations are observed). Many infrared techniques have been used for their ease of sample preparation and high sensitivity. These techniques are: diffuse reflectance infrared Fourier transform spectroscopy (DRIFTS), attenuated total internal reflectance (ATR) spectroscopy, and the thermal desorption techniques; thermogravimetry Fourier transform infrared (TG-FTIR) and headspace analysis gas-phase infrared spectroscopy (HAGIS).

### **2.2.5.1 Diffuse Reflectance Infrared Fourier Transform Spectroscopy (DRIFTS)**

Diffuse reflectance is based on the interaction of an incident infrared beam focused on a fine particulate material. There are three types of reflection that this incident beam can undergo (Figure 2-3). Firstly, the radiation can be reflected at an angle equal to the angle of the incident beam without penetrating into the particle. This reflection mode is known as true specular reflection and is a function of the refractive index and absorptivity of the material. Secondly, the beam can undergo multiple reflections without penetrating the sample and emerge at a random angle relative to the incident beam. This mode is termed diffuse specular reflectance and is a function of the refractive index of the sample. Finally, the beam can penetrate into one or more particles and scatter from the sample matrix. This mode is known as true diffuse reflectance and contains information about the absorption characteristics of the sample material.

Quantitative measurements can be obtained using the Kubelka-Munk model, which relates sample concentration to the intensity of the measured infrared spectrum similarly to Beer's Law. Linear relationships are predicted only for samples that are highly diluted in a non-absorbing matrix such as KBr. Samples must also be prepared to a uniform fine size and the sample thickness must be

## Chapter 2 – Literature Review

thick relative to the wavelength, approximately 3 mm. The main restrictions to quantitative analysis with this technique are control of particle size and matrix reflectivity.

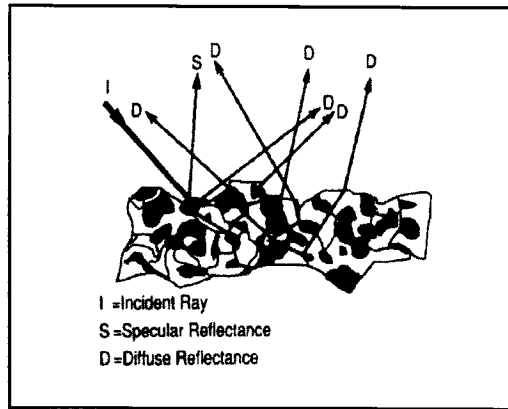


Figure 2-3 Schematic of specular and diffuse reflectance (Baulsir and Tague)<sup>42</sup>.

Diffuse reflectance spectra have been reported for galena, sphalerite and pyrite treated with potassium alkylxanthates<sup>43</sup>. The results indicated the presence of lead(II) alkylxanthate on the surface of galena and dialkyl dixanthogen on pyrite surfaces. The adsorbed species can easily be determined by comparison with the synthesized form (i.e., surface lead(II) ethylxanthate compared to solid lead(II) ethylxanthate). Contini et al.<sup>44</sup> used DRIFTS to monitor the adsorption of mercaptobenzothiazoles onto galena at concentrations from  $10^{-5}$  to  $10^{-3}$  M for 0.1 g mineral. Although they used great care in controlling particle size and maintaining the matrix effects constant, only qualitative information was reported without any attempt at quantification.

### 2.2.5.2 Attenuated Total Internal Reflectance (ATR) Spectroscopy

When infrared radiation enters an infrared transmitting material (ATR crystal) having a high refractive index under certain geometries, it will be completely internally reflected. The internal reflectance creates an evanescent wave, which extends beyond the surface of the crystal into the sample held in contact with the crystal (Figure 2-4). If the sample absorbs energy in the infrared region, the

## Chapter 2 – Literature Review

evanescent wave will be attenuated. For internal reflectance to occur, the incident angle of radiation must be larger than the critical angle,  $\theta_c$ , defined as:

$$\theta_c = \sin^{-1} \frac{n_2}{n_1} \quad \text{Equation 2-1}$$

where  $n_1$  is the refractive index of the ATR crystal and  $n_2$  is the refractive index of the sample. Materials of high refractive index (i.e. ZnSe,  $n = 2.4$ ) are generally chosen for the ATR crystal to lower the critical angle. Because of the exponential decay of the evanescent wave, ATR is generally insensitive to sample thickness and can therefore be used to analyze thick or highly absorbing samples.

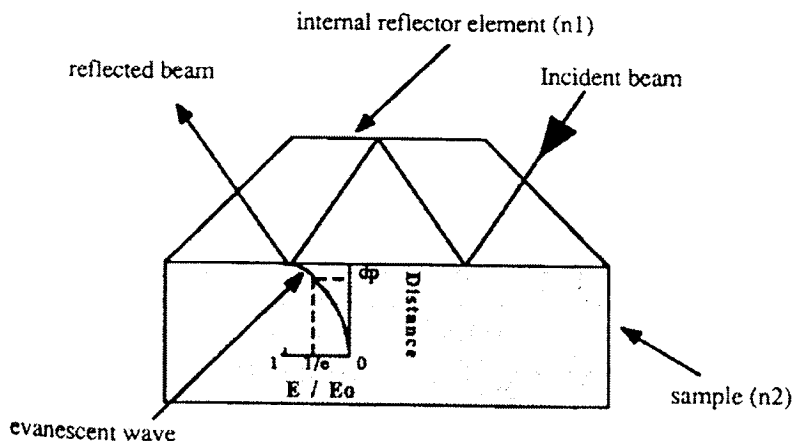


Figure 2-4 Optical diagram of an ATR prism showing the amplitude decay of the evanescent wave (Cases and De Donato)<sup>46</sup> where  $E_0$  and  $E$  are the amplitudes of the electric field at the ATR surface and in the sample, respectively.

Applications of FTIR-ATR spectroscopy have been extensively documented for xanthate adsorption on sulphide mineral surfaces. In ethyl xanthate treatment of galena (PbS), lead xanthate is found at monolayer coverage levels<sup>45,46</sup>. Diethyl dioxanthogen was reported on pyrite ( $\text{FeS}_2$ ), pyrrhotite ( $\text{Fe}_{1-x}\text{S}$ ), and chalcopyrite ( $\text{CuFeS}_2$ )<sup>47</sup>. Iron xanthate and copper xanthate were found to coexist with diethyl dioxanthogen on pyrite and chalcopyrite, respectively, as monolayers<sup>45,47</sup>. After Cu activation, copper(I) xanthates were found on all three minerals<sup>47</sup> as was the case for Cu-activated sphalerite ( $\text{ZnS}$ )<sup>48</sup> and sulphidized copper surfaces<sup>49</sup>. A ferric



## Chapter 2 – Literature Review

---

hydroxy-xanthate complex was observed on the surface of iron ( $\text{Fe}^{2+}$ ) activated sphalerite<sup>17</sup>.

Molecular orientations of adsorbed xanthate can be determined by using the dichroic ratio of polarized FTIR-ATR, which is defined as:

$$D = \frac{A_s}{A_p} \quad \text{Equation 2-2}$$

where  $A_s$  and  $A_p$  are the experimentally measured absorption values with perpendicular and parallel polarized beams, respectively (Figure 2-5).

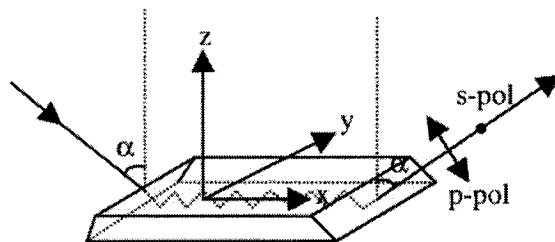


Figure 2-5 IR beam direction and polarization in ATR setup (Larsson et al.)<sup>50</sup>.

The measured absorbance reflects the average tilt angle,  $\gamma_0$ , for all molecules or the average tilt angle for a molecular transition moment on the surface. The tilt angle is related to an order parameter,  $S$ , through the standard definition for liquid crystals as follows<sup>51</sup>:

$$S = 1.5 \cos^2 \gamma - 0.5 \quad \text{Equation 2-3}$$

The relationship between the order parameter,  $S$ , and the surfactant orientation is shown in Figure 2-6. Perfect order is observed at  $\gamma = 0^\circ$  and  $S = 1$ , full disorder is observed at  $\gamma = 54.7^\circ$ ,  $S = 0$  and perfect planar orientation at  $\gamma = 90^\circ$ ,  $S = -0.5$ .

## Chapter 2 – Literature Review

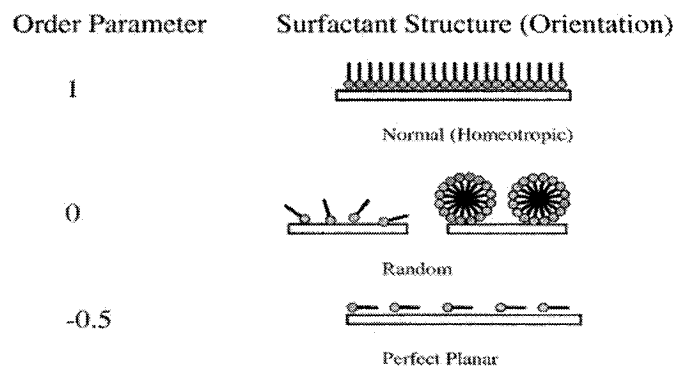


Figure 2-6 Schematic representation of surfactant orientation relative to order number (Singh et al.)<sup>51</sup>.

Studies of heptylxanthate adsorption onto ZnS have shown the tilt angle to be  $44^\circ \pm 5^\circ$ , which suggests a bridging coordination with the mineral surface as shown in Figure 2-7.

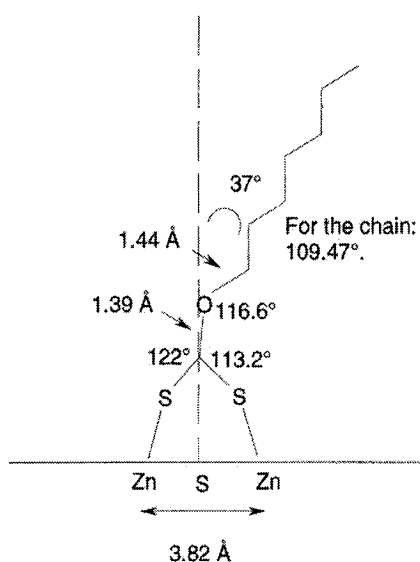


Figure 2-7 Representation of heptylxanthate bridging coordination to a ZnS surface with resulting tilt angle of  $37^\circ$  (Larsson et al.)<sup>50</sup>.

### 2.2.6 Raman Spectroscopy

In Raman spectroscopy, the sample is irradiated with a monochromatic light source (often an Nd:YAG laser emitting in the near infrared region at 1064 nm),

## Chapter 2 – Literature Review

the molecule is excited to an unstable state and immediately returns to a lower energy state, emitting a photon. Most molecules return to the ground state and scatter the light with unchanged wavelength (Rayleigh scattering) but some molecules return to an excited vibronic state (Figure 2-8) sending a photon with lower energy than the incoming photon (Raman scattering). As in infrared, the energy difference becomes vibrational energy in the molecule.

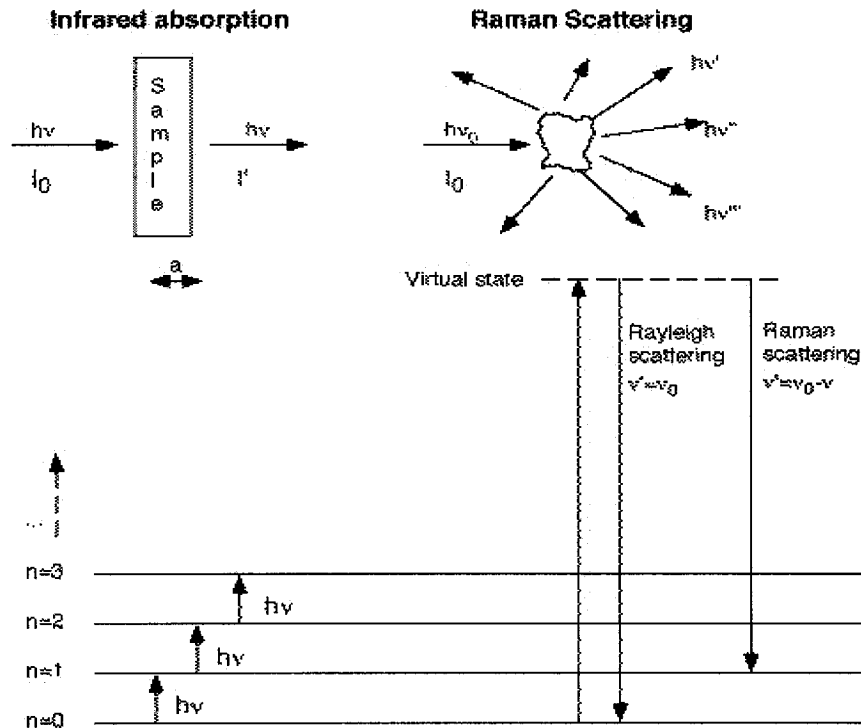


Figure 2-8 Raman scattering processes compared to infrared absorption (Kariis<sup>52</sup>).

Surface enhanced Raman spectroscopy (SERS) is obtained when the surface area of the sample is increased using resonance and allows for surface layers at the sub-monolayer level to be characterized. Woods and coworkers<sup>53-55</sup> have used SERS to observe the interaction of common collectors with copper, silver and gold surfaces. These surfaces have been chosen because of their high response to SERS. They were able to determine chemisorption properties; xanthate bonded to silver atoms through its sulphur atoms, mercaptobenzothiazole (MBT) chemisorbed through its exocyclic sulphur atom and a surface metal atom, and

## **Chapter 2 – Literature Review**

---

dialkyldithiophosphate (DTPI) was oxidized to its disulphide on gold, chemisorbed through charge transfer onto silver, and did not have a SERS spectra on copper although the presence of DTPI was observed on the surface of copper sulphide by Raman spectroscopy. The DTPI results clearly show a possible problem with the use of SERS. In addition, metal surfaces do not always behave in the same manner, in terms of chemisorption, as metal sulphides. It is also impossible to quantitatively determine collector adsorption onto plant samples, as specially prepared surfaces are needed to perform SERS analysis.

### **2.2.7 UV-Visible Spectroscopy**

The absorption of ultraviolet (UV) or visible radiation by molecules corresponds to the excitation of outer electrons. Quantitative analysis is based on the Beer-Lambert law, which states that the absorbance is directly proportional to the path length,  $l$ , and the concentration,  $c$ , of the absorbing species expressed as follows:

$$A = \epsilon lc \qquad \text{Equation 1-1}$$

where  $\epsilon$  is the proportionality constant known as the absorptivity. An absorbance spectrum shows absorption bands belonging to different structural groups within the molecule. For example, ethyl xanthate has a UV absorbance band at 301 nm, while its decomposition products ethyl monothiocarbonate, ethyl perxanthate, and diethyl dixanthogen have absorbance bands at 225, 346, and 238 and 288 nm, respectively<sup>59</sup>. This method is commonly used to determine the concentration of collector that is adsorbed by comparing the initial and final solutions after contact with the mineral (i.e., the adsorbed concentration is obtained by difference). UV-Visible spectroscopy may be used with extraction into a solvent to determine adsorbed collector concentrations.

## **Chapter 2 – Literature Review**

---

### **2.2.8 Thermal Desorption Methods**

Thermal methods of analysis are techniques in which a property of a sample is monitored versus time or temperature<sup>57</sup>. Many of the thermal techniques described below require the use of combined techniques (e.g. TG-FTIR, TG-MS) for the determination of adsorbed reagents.

#### **2.2.8.1 Differential Thermal Analysis (DTA)**

The term “differential” refers to the measurement of a difference in a property between the sample and a reference. Therefore, differential thermal analysis measures the difference in temperature between a sample and a reference. Howe and Pope used this technique and reported a limit of detection of 0.1 mg/g for n-dodecylamine and sodium oleate adsorbed on titanium dioxide<sup>58</sup>. They suggest that this technique should be applicable to any adsorbed reagent since its heat of combustion may be determined in a separate experiment. This may not hold, however, for xanthate type collectors because they tend to decompose into different products depending on the species formed upon adsorption<sup>59</sup>.

#### **2.2.8.2 Selective Oxidation / Combustion Analysis**

Quantitative analysis of collector on mineral surfaces is obtained through combustion, effectively oxidizing the hydrocarbon collectors in a high-purity oxygen stream over a given temperature range followed by conversion to carbon dioxide by catalysis and IR detection of the evolved carbon dioxide<sup>9,40</sup>. Pugh and Husby applied the technique to long-chain amines, fatty acids and xanthates and reported the possible determination of carbonates on fluorite and galena<sup>9</sup>. Detection limits ranged from 70 to 200 g/t. In phosphate ore processing, Miettinen et al.<sup>40</sup> reported the detection of 20 g of sarcosine-type collector per tonne of ore.

#### **2.2.8.3 Thermogravimetry Fourier Transform Infrared (TG-FTIR) and Mass Spectrometry (TG-MS)**

In thermogravimetry, it is the mass of the sample that is monitored against time or temperature. Often, derivative thermogravimetry (DTG) is used because the derivative function enhances the steps in the TG curve making them easier to

## **Chapter 2 – Literature Review**

---

identify. On its own, TG would not be very useful in quantifying collector adsorption because of its inability to differentiate between various desorption products giving only information on the total amount of adsorbed organics. When it is used in conjunction with an organic analysis tool such as FTIR or MS, however, it can be used for quantitative determination of adsorbed reagents. Fisher, Dunn and coworkers have compared TG-FTIR and TG-MS in the determination of collectors and frothers on activated carbon from gold processing plants<sup>60-62</sup>. Their results show that TG-MS is able to monitor evolved gases as a function of temperature while only the major components were readily identifiable by TG-FTIR. In analysing complex gaseous mixtures, the two techniques performed very poorly and a thermal desorption – pyrolysis – GC – MS (TD-py-GC-MS) analysis technique was suggested as an alternative<sup>63</sup>. One of the problems with quantitative TG-FTIR or TG-MS is condensation of the gases in the transfer line between the two instruments. Jackson and Rager have reported that operating the transfer line under reduced pressure results in minimal sample carryover and reduced material trapping in the transfer line<sup>64</sup>. In fact, using reduced pressure can yield information on the sample structure and the thermal decomposition process.

### **2.2.8.4 Headspace Analysis Gas-Phase Infrared Spectroscopy (HAGIS)**

Headspace analysis gas-phase infrared spectroscopy is an indirect technique for the analysis of surfactants adsorbed onto solid surfaces<sup>65,66</sup>. The method works by desorbing the surfactant into gas-phase with heat. The HAGIS cell (Figure 2-9) is constructed from glass and is equipped with two vacuum stopcocks for purging of the cell with different atmospheres (i.e., N<sub>2</sub>, CO<sub>2</sub>-free air, etc). The cell is closed by two Teflon end-caps with removable KRS-5 windows. The sample is placed in a stainless steel sample boat that is connected to a temperature controller. The infrared beam is not directed on the sample itself but rather on the headspace above the sample boat where only gas-phase species will be present.

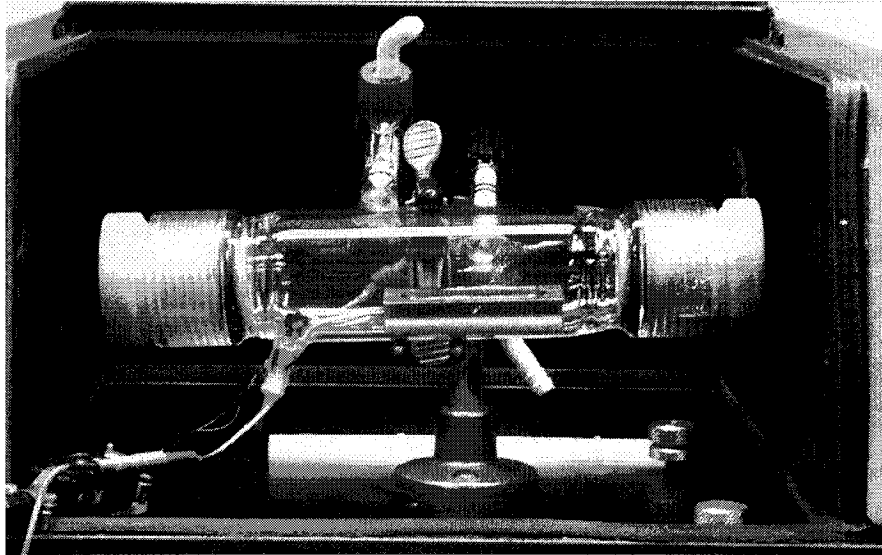


Figure 2-9 Photo of loaded HAGIS cell (Lascelles et al.)<sup>67</sup>.

Sample sizes can range from 20mg to 5g with the current sample boat. Because the concentration of the gas-phase species is directly related to the amount of sample, simply changing the sample size can vary the effective detection limit, therefore allowing for collector dosages in the range used in plant practice. Clear advantages of the method are the minimal sample preparation, which involves a gravity or vacuum filtration (and, if necessary, drying and sampling as in standard practice for assaying), and freedom from solid matrix effects: minerals do not need to have similar physical properties to be compared.

Vreugdenhil et al.<sup>66</sup> have reported the following for ethylxanthate adsorption on sulphide mineral surfaces: dixanthogen at low surface coverage for chalcopyrite and pyrrhotite with the presence of metal xanthate at higher collector dosages; lead xanthate was the only species detected on the surface of galena while only dixanthogen was observed on pyrite surfaces; xanthate collector was not significantly adsorbed onto unactivated sphalerite. All of these findings support previous conclusions<sup>68</sup>.

## **Chapter 2 – Literature Review**

---

Quantitative analysis using the HAGIS technique has not yet been explored. The experimental set-up does lend itself to quantification according to Beer's law as a matrix effect is absent, the cell pathlength is fixed and there is no transfer of the evolved gases to other instruments. The simplicity and affordability of the technique make it a very attractive tool for the analysis of reagent adsorption in mineral processing systems.

### **2.3 Conclusions**

The main requirements can be summarized as follows: the ability to give information on the adsorption mechanism, ease of use and amenability to quantitative analysis at dosages comparable to industry. ToF-SIMS is a candidate because it is able to determine reagent adsorption at very low levels. The technique is sensitive to matrix effects, however, and only relative quantification is possible. It is noted that the analysis is on a particle at-a-time basis and generating the number of mineral grains to meet statistical criteria is time consuming. Similarly, the combination of synchrotron radiation with XPS (SRXPS) allows for the detection of submonolayer coverage of adsorbed reagents and gives information on the adsorption mechanism. The technique is also time consuming and requires the access to a synchrotron radiation source. Traditional infrared spectroscopy techniques such as DRIFTS and ATR have been widely utilized in identifying the adsorption mechanism of a range of collectors. In DRIFTS, the need to control particle size and the matrix effects make it almost unusable for quantitative analysis. ATR is very useful for determining surfactant orientation and structure, but has a high detection limit and is therefore not appropriate for analysing process samples. Infrared techniques such as TG-FTIR or HAGIS show promise in quantitative analysis, because matrix effects are largely eliminated as the adsorbed reagent is thermally desorbed prior to analysis. The simplicity of the HAGIS technique makes it very attractive for quantitative analysis and is the technique that will be explored.



# 3 Quantitative Spectroscopy

A standard text is by Smith “Quantitative Spectroscopy: Theory and Practice”<sup>15</sup>. The book covers quantitative analysis using spectroscopy, specifically infrared spectroscopy, in great detail. As we are attempting to use an infrared technique (HAGIS) to perform quantitative analysis, the tools presented by Smith are appropriate and will be reviewed.

### 3.1 Beer’s Law

Beer’s law identifies the relationship between the amount of light absorbed by a sample and the concentration of the absorbing species. It is the basis of quantitative spectroscopy.

When a sample of absorbent material is subjected to monochromatic light of wavelength  $\lambda$  and initial intensity  $I_0$ , the light leaves the sample with a lower intensity  $I$  due to the sample absorption (Figure 3-1). Absorption of the incident light is due to three types of interaction that the photons may undergo with the molecules. In elastic collisions, there is no net transfer of energy between the photon and the molecule. These collisions result in Rayleigh scattering.

## Chapter 3 – Quantitative Spectroscopy

---

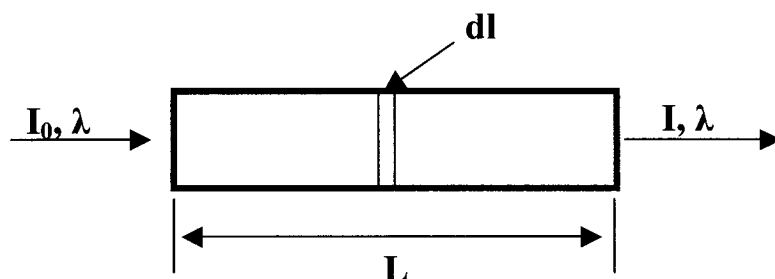


Figure 3-1 Absorbance of photons by a sample (Smith)<sup>15</sup>.

Inelastic collisions result when energy is exchanged between the particles. In the case of photons interacting with molecules, these collisions are called Raman scattering. The amount of energy lost by the photon,  $E_v$ , is characteristic of the molecule involved. As in infrared spectroscopy, a Raman spectrum is obtained when the intensity and wavenumber of the photons are plotted. Raman spectra measure the vibrational energy levels of a molecule and may be used for quantitative chemical analysis.

When the collision is totally inelastic, absorbance takes place. The wavenumber of the photon that is absorbed and the absorption intensity depend upon the molecule involved. Chemical information can be derived from the absorbance spectrum. The total amount of light absorbed by a sample is equal to the total number of photons that undergo totally inelastic collisions with molecules. The depletion of photons leaving the sample is the result of absorption.

The amount of light absorbed across a length of the sample  $dl$  can be denoted by  $dI$  (Figure 3-1). Collisions are proportional to the number of photons hitting the sample. The concentration of absorbing species in distance  $dl$  is denoted by  $c$  and the intensity of light by  $I$ . The thicker the sample,  $dl$ , the more photons are absorbed because of the increased number of molecules. The following proportionality is obtained for the light adsorbed in  $dl$ :

## Chapter 3 – Quantitative Spectroscopy

---

$$-dI \propto I c dl \quad \text{Equation 3-1}$$

The negative value for  $dI$  indicates that the light beam decreases in intensity as it goes through the sample. Every molecule has a specific percentage of totally inelastic collisions that are possible. The number of totally inelastic collisions determines the amount of light that will be absorbed. This number is called the absorptivity ( $\epsilon$ ). Because the absorptivity depends on the identity of the molecule, it functions as a proportionality constant resulting in Equation 3-2. The qualitative relationship thus becomes quantitative.

$$-dI = \epsilon I c dl \quad \text{Equation 3-2}$$

where  $\epsilon$  is the absorptivity of the analyte molecule at wavelength  $\lambda$ . If we rewrite the equation in terms of intensity, we obtain

$$-\frac{dI}{I} = \epsilon c dl \quad \text{Equation 3-3}$$

Integrating between  $I_0$  and  $I$ , and over the pathlength  $L$ , we obtain

$$\ln \frac{I_0}{I} = \epsilon c l \quad \text{Equation 3-4}$$

which is the basis of Beer's law. The traditional way to express Beer's law uses base 10 logarithms and this is done by simply including the 2.303 factor ( $\ln(10) = 2.303$ ) in the absorptivity which gives

$$\log \frac{I_0}{I} = \epsilon c l \quad \text{Equation 3-5}$$

## Chapter 3 – Quantitative Spectroscopy

---

A new quantity termed absorbance,  $A = \log \frac{I_0}{I}$ , was defined to simplify the equation. Beer's law therefore takes on the commonly expressed form:

$$A = \epsilon lc \quad \text{Equation 1-1}$$

Beer's law indicates that the amount of light absorbed by a sample depends, in linear fashion, on the concentration of the analyte, the sample thickness and its absorptivity. Because of the linear relationship, the peak height or area of an analyte's absorbance band will vary linearly with concentration.

Transmittance,  $T = \frac{I}{I_0}$ , is also commonly used in presenting infrared data. The values can vary from 1, when  $I = I_0$  to 0 when  $I = 0$  and spectra are therefore often plotted as percent transmission ( $\%T = T \times 100$ ). Transmittance is related to absorbance as follows:

$$A = \log \frac{1}{T} \quad \text{Equation 3-6}$$

By substituting Equation 3-6 into Beer's law, we obtain the following relationship for transmittance

$$T = 10^{-\epsilon c L} \quad \text{Equation 3-7}$$

Because the relationship between transmittance and analyte concentration is not linear, transmittance spectra are inappropriate for use in quantitative analysis.

## Chapter 3 – Quantitative Spectroscopy

---

It is important at this point to consider the factors that may affect the absorbance. Temperature is one. Quantum mechanics show that temperature effects are most important when low energy transitions are being monitored<sup>15</sup>.

Another factor, particularly in quantitative spectroscopy, is the matrix effect. The composition of a sample influences the interactions with the molecules, which impacts on the resulting absorbance values. The concentration of a sample will also impact its chemical environment. The crowding of the analyte molecules results in skewed absorptivities due to molecular interactions. This is the reason why Beer's law becomes non-linear at high concentrations. Although temperature has little effect on the absorbance of the analyte sample, it does affect the sample matrix. Higher temperatures result in increased molecular collisions altering the strength of intermolecular interactions. Finally, the effect of pressure is very small on solid and liquid samples but becomes an important variable in gas samples.

### 3.2 Gas Phase Quantitative Spectroscopy

As mentioned, the effect of pressure becomes important when attempting to use quantitative spectroscopy in the gas phase. The pressure effect may be derived using the ideal gas law,  $PV = nRT$ . If we take the concentration,  $c$ , to be the number of moles divided by the volume ( $c = \frac{n}{V}$ ) we can derive the ideal gas law expressed in terms of concentration

$$c = \frac{P}{RT} \qquad \text{Equation 3-8}$$

We can also express Beer's law in terms of analyte concentration (Equation 3-9) and obtain Beer's law for the Gas Phase (Equation 3-10).

## Chapter 3 – Quantitative Spectroscopy

---

$$c = \frac{A}{\epsilon l} \quad \text{Equation 3-9}$$

$$A = \frac{P\epsilon l}{RT} \quad \text{Equation 3-10}$$

The resulting equation indicates that absorbance values are dependent on the pressure and temperature of the sample. In order to obtain proper calibrations, it is important to keep the pressure and temperature of the standard and unknown samples the same.

### 3.3 Analysis Methods

In analyzing samples, the signal-to-noise ratio (SNR) is an indication of how “good” the data are. A high SNR means better quality data. In order to maximize the SNR, random errors must be kept to a minimum. Random errors are caused by variables over which we have no control such as fluctuations in electrical voltage. As implied, random errors can be either positive or negative. Performing multiple experiments and averaging minimizes random errors. This is the reason why scans are co-added in spectroscopy.

Another method of increasing the SNR is to use the peak maximum when using peak height for calibrations. The peak maximum will always have the highest SNR. The use of peak areas will increase the SNR further as a larger absorbance value results. In the peak height versus peak area debate, Smith mentions that when peak height is measured, only one of many data points in a peak whose absorbance is sensitive to the analyte concentration is used in the analysis. If anything causes accuracy to be compromised, the entire calibration is thrown off. Peak area, on the other hand, is the addition of the absorbances of many data points, e.g., from 2270 to 2195 there are 40 different wavenumbers. By using more data points, calibration is less sensitive to error in any specific data point. In general, peak areas produce more robust and accurate calibrations because they

## **Chapter 3 – Quantitative Spectroscopy**

---

are not as dependent on a single data point. There are some applications, however, where peak height works better than peak area. A rule of thumb is to try peak area first; and if the calibration is not as good as expected, try peak height.

### **3.3.1 Single Analyte Analysis**

The calibration and prediction of a single component is easily carried out with Beer's law. A linear plot of absorbance versus concentration indicates that the system follows Beer's law. These plots should not be forced through zero. Once we have a calibration, the concentration of the unknown is predicted using Equation 1-1 where the slope of the linear regression is equal to the absorptivity multiplied by the cell pathlength.

When performing a linear regression (least squares fitting) on a set of data, the following assumptions are made:

1. The equation used perfectly describes the data. In our case, we assume that the system follows Beer's law and that absorbance is affected by  $\epsilon$ ,  $l$  and  $c$  only. We therefore need to ensure that any other variables such as temperature and pressure are well controlled.
2. The equation being fitted must be linear since absorptivity and the pathlength are assumed to vary linearly with absorbance.
3. All the error in the data is random. It is assumed that there is no systematic error in either the absorbance or the concentration data. This may not be realistic, and it is more reasonable to assume that the systematic error is significantly less than the random error.
4. The shape and extent of the scatter has to be the same for all y-axis data. The errors should follow a Gaussian distribution and the standard deviation should be the same for each sample.
5. There is no error in the x-axis data. Because error-free data do not exist, this assumption is automatically violated. The solution is to always use the data with the smallest error as the x-axis data. In the case of Beer's

## Chapter 3 – Quantitative Spectroscopy

---

law, the error in the concentration is usually an order of magnitude larger than the error in the absorbance data. One should therefore plot concentration versus absorbance, commonly known as an inverse Beer's law plot for quantitative spectroscopy.

The following sampling practice is proposed:

1. Use maximal accuracy in preparing standards to keep error at a minimum.
2. Take two independent measurements of each standard. They should be identical.
3. Subtraction of the two spectra obtained should give a reasonably flat residual with noise only.
4. Examine the spectra and determine the peaks that are dependant on concentration.
5. Measure absorbance and plot the calibration line. Examine the plot to ensure linearity and calculate the slope. The quality and robustness of the curve should be verified. The quality of a model (how well it fits the data) is described by

$$R = \left( \frac{SSR}{SST} \right)^{1/2} \quad \text{Equation 3-11}$$

where SSR is the modeled variance ( $SSR = \sum_i (Y_i - \bar{Y})^2$ ) and SST is the total variance ( $SST = \sum_i (Y_i - \bar{Y})^2$ ). A value of unity for R ( $R=1$ ) described a perfect model.

The robustness of the curve is described by *F for Regression*

$$F = \frac{SSR (n - m - 1)}{SSE m} \quad \text{Equation 3-12}$$



### **Chapter 3 – Quantitative Spectroscopy**

---

where  $n$  is equal to the number of data points and  $m$  the number of independent variables. The larger is the  $F$ , the more robust is the calibration.

6. Obtain the spectrum of the unknown sample and calculate the unknown concentration using the calibration curve.

The following steps may help to limit common experimental errors.

1. The standards must bracket the expected concentration of the unknown. It is inappropriate to extrapolate the calibration model.
2. When preparing the calibration curve, the actual experimental components should be used; not pure reagents (e.g., technical grade sodium isopropyl xanthate instead of a purified xanthate).
3. The standards should be run in random order to ensure that sample order has no effect on results.
4. The minimum number of standards to run is  $2n+2$  where  $n$  is the number of components to be analyzed. For a single component, at least four standards should be run.
5. Occasionally obtain the spectrum of the sample cell with no sample present to check for contamination.
6. Only use absorbance bands that are less than 0.8 because Beer's law is usually not obeyed at high absorbance.
7. Ensure that there is no interaction between the sampling cell and the sample.
8. Keep physical conditions, such as temperature and pressure the same for standards and samples. In the case of mineral samples, this may include particle size distribution.
9. Use the same instrumental parameters (e.g., number of scans, resolution, spectral range) for all samples.
10. Perform as little spectral manipulation as possible. They are difficult to reproduce from one spectrum to another.

## Chapter 3 – Quantitative Spectroscopy

---

11. Always use the same sampling cell and cell window material (i.e., if the standards were taken with KRS-5 windows (TlCl) do not change to KBr for the unknowns).
12. Double-check an established calibration periodically by using a new standard and comparing to the calculated concentration.

### 3.3.2 Multiple Component Analysis

In quantifying two or more components in an unknown sample, we may use the least squares method or chemometric / factor analysis techniques. When each component has a band/peak that is independent of the others, the procedure for single component analysis may be followed for all components. If on the other hand there are no independent bands, the additive character of Beer's law may be used ( $A_t = A_a + A_b + A_c$ ). Because we are left with as many unknowns as we have components, we need to have the same number of bands to analyze. In a 3-component system, we then solve for

$$\begin{aligned} A_1 &= \varepsilon_{1a}lc_a + \varepsilon_{1b}lc_b + \varepsilon_{1c}lc_c \\ A_2 &= \varepsilon_{2a}lc_a + \varepsilon_{2b}lc_b + \varepsilon_{2c}lc_c \\ A_3 &= \varepsilon_{3a}lc_a + \varepsilon_{3b}lc_b + \varepsilon_{3c}lc_c \end{aligned} \quad \text{Equation 3-13}$$

which may be written as the Beer's law matrix

$$\begin{pmatrix} A_1 \\ A_2 \\ A_3 \end{pmatrix} = \begin{pmatrix} \varepsilon_{1a} & \varepsilon_{1b} & \varepsilon_{1c} \\ \varepsilon_{2a} & \varepsilon_{2b} & \varepsilon_{2c} \\ \varepsilon_{3a} & \varepsilon_{3b} & \varepsilon_{3c} \end{pmatrix} \begin{pmatrix} l \\ l \\ l \end{pmatrix} \begin{pmatrix} c_a \\ c_b \\ c_c \end{pmatrix} \quad \text{Equation 3-14}$$

$\mathbf{A} = \mathbf{ELC}$

#### 3.3.2.1 Classical Least Squares (K Matrix) Method

In Classical Least Squares (CLS), the pathlength and absorptivity matrices are combined into a single matrix called  $\mathbf{K}$  ( $\mathbf{K}=\mathbf{EL}$ ). The matrix equation for Beer's law then becomes

## Chapter 3 – Quantitative Spectroscopy

---

$$\mathbf{A} = \mathbf{KC} \quad \text{Equation 3-15}$$

By determining the K matrix, a calibration is obtained. Because we are working with matrices, we may “square” the C matrix and use its inverse to calculate K as follows:

$$\mathbf{K} = \mathbf{AC}^T(\mathbf{CC}^T)^{-1} \quad \text{Equation 3-16}$$

This equation is the matrix definition of a least squares fit. Once K is known, we can predict the unknown concentrations with the following equation:

$$\mathbf{C}_{\text{unk}} = (\mathbf{K}^T\mathbf{K})^{-1}\mathbf{K}^T\mathbf{A}_{\text{unk}} \quad \text{Equation 3-17}$$

where  $C_{\text{unk}}$  is the component concentration in the unknown sample and  $A_{\text{unk}}$  is the absorbance of the unknown sample. By calculating C this way, all the unknown concentrations are determined at once.

### 3.3.2.2 Inverse Least Squares (P Matrix) Method

Similarly to CLS where the absorptivity and the pathlength matrices are combined into the K matrix, in the P matrix method they are combined and inverted. The inverse matrix form of Beer’s law is written as follows:

$$\mathbf{C} = \mathbf{PA} \quad \text{Equation 3-18}$$

where P is easily determined by applying the least squares method to perform a calibration as follows:

$$\mathbf{P} = \mathbf{CA}^T(\mathbf{AA}^T)^{-1} \quad \text{Equation 3-19}$$

The real practicality of this technique is that C is therefore easily obtained by using Equation 3-19.

Some advantages of the inverse least squares method are that it is not necessary to know the concentration of all the molecules in standard samples and interferences,

### **Chapter 3 – Quantitative Spectroscopy**

---

impurities and baseline effects are handled well. It is also easily used for a wide variety of applications.

The most important disadvantage is that the number of standards must be greater than the number of absorbances, limiting the number of wavenumbers that can be used. It is often difficult to find an optimum set of wavenumbers and the increased number of standards to be processed becomes time consuming.

# 4 Experimental Techniques

## 4.1 Introduction

Reagent adsorption was determined by two methods: indirectly by solution analysis either through ultraviolet-visible spectroscopy (UV-Vis) or liquid chromatography combined with mass spectrometry (LC-MS) or directly with Headspace Analysis Gas-phase Infrared Spectroscopy (HAGIS). Batch flotation experiments were conducted with a Denver flotation cell.

## 4.2 UV-Visible Spectroscopy

The absorption of ultraviolet (UV) or visible radiation by molecules corresponds to the excitation of outer electrons. An absorbance spectrum shows absorption bands belonging to different structural groups within the molecule. For example, ethyl xanthate has a UV absorbance band at 301 nm, while its decomposition products ethyl monothiocarbonate, ethyl perxanthate, and diethyl dixanthogen have absorbance bands at 225, 346, and 238 and 288 nm, respectively<sup>56</sup>.

UV-Vis is used for the indirect determination of adsorbed reagents. Calibration curves were prepared for sodium isopropyl xanthate and diphenylguanidine with prepared standard solutions. In Chapter 5, the adsorbed xanthate concentrations are calculated

## **Chapter 4 – Experimental Techniques**

---

from the area of the xanthate peak at 301 nm. The diphenylguanidine peak present at 254 nm above pH 11 is used in Chapter 6.

### **4.3 Liquid Chromatography – Mass Spectrometry**

In liquid chromatography, a sample (dissolved in a liquid mobile phase) is forced through an immiscible stationary phase. The components in the sample will be retained, at different retention levels, by the stationary phase. Components that are strongly retained by the stationary phase will move slowly through the column while components that are weakly held travel faster. If the phases are chosen properly, each component in a sample will have a discrete emerging band that can be analyzed quantitatively (e.g., by mass spectrometry).

In mass spectrometry, the components of a sample are converted into rapidly moving gaseous ions and separated on the basis of their mass-to-charge ratios. A very small amount of sample is volatilized at the inlet. Electrons, ions, molecules or photons bombard the sample into charged components, and they are detected with an electron multiplier and their mass analyzed. Mass spectrometry is often used for qualitative or quantitative analysis in tandem with gas or liquid chromatography.

The LC-MS data reported in Chapter 6 are from solution analysis conducted by MAXXAM Analytics Inc. The samples were sealed in polypropylene test tubes and refrigerated until sent for analysis.

### **4.4 Fourier Transform Infrared Spectroscopy (FTIR)**

Infrared spectroscopy measures the absorption of incident infrared radiation as it passes through a sample. Infrared radiation is absorbed when a molecule undergoes a net change in dipole moment as a consequence of vibrational or rotational motion. In order to be infrared active, molecules must have a dipole moment. The energy of the vibration and hence the wavenumber of the radiation absorbed is determined by the infrared active

## Chapter 4 – Experimental Techniques

---

components of the molecule. For example, CO<sub>2</sub> will absorb at 2330 cm<sup>-1</sup> due to the asymmetric stretching of the molecule (Figure 4-1).



Figure 4-1 Asymmetric stretching of a CO<sub>2</sub> molecule.

In Fourier transform infrared, the infrared source beam is split into two beams whose path lengths are varied periodically to give interference patterns. The Fourier transform is used for data processing. The advantage of FTIR is better signal-to-noise ratio (or rapid scanning), high resolution (< 0.1 cm<sup>-1</sup>) and accurate and reproducible frequency determinations.

### 4.5 Headspace Analysis Gas-Phase Infrared Spectroscopy (HAGIS)

The HAGIS cell (Figure 4-2) developed by Dr. A. J. Vreugdenhil<sup>69</sup> is constructed from glass and is equipped with two vacuum stopcocks for purging with different atmospheres (i.e., N<sub>2</sub>, CO<sub>2</sub>-free air, etc). The cell is closed by two Teflon end-caps with removable KRS-5 windows. The sample is placed in a stainless steel sample boat connected to a temperature controller. The infrared beam is not directed on the sample but rather on the headspace above the boat where only gas-phase species will be present.

Sample sizes can range from 0.1 mg to 5 g with the current set-up. Because the concentration of the gas-phase species is directly related to the amount of sample, simply increasing the sample mass can reduce the effective detection limit. Clear advantages of the method are the minimal sample preparation, which involves gravity or vacuum filtration and drying and sampling as in standard practice for assaying, and the freedom from solid matrix effects: minerals do not need to have similar physical properties to be compared.

## Chapter 4 – Experimental Techniques

---

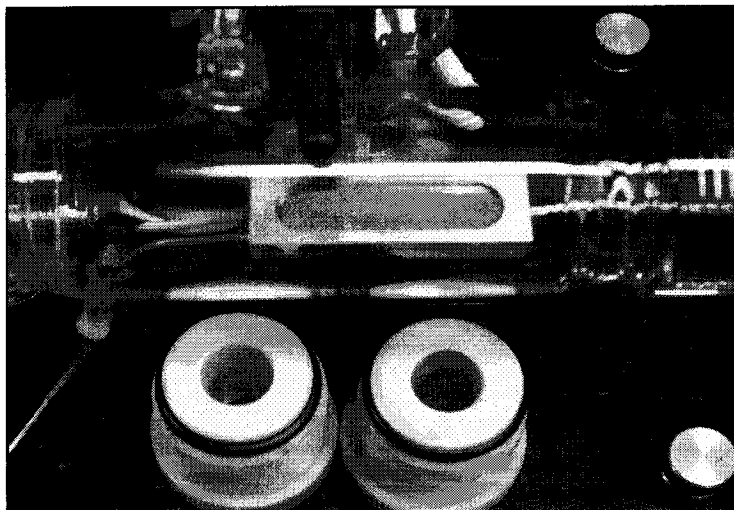


Figure 4-2 HAGIS cell (open) showing filled sample boat and Teflon endcaps.

For our purposes, 0.1 mg to 3 g samples were used and the cell was closed and purged with dry air or nitrogen for 1 minute. A background spectrum was obtained. The heating temperature was chosen according to the reagent to be analyzed. The temperature should lie approximately 20°C above the boiling point of the reagent to ensure desorption will take place. The temperature is maintained for 10 to 120 minutes and the sample spectrum obtained. The HAGIS cell was used with the Bruker IFS-66 FTIR spectrometer and a nitrogen cooled MCT detector. Both the background and sample spectra included 500 scans.

### 4.6 Batch Flotation Tests

Batch flotation tests were conducted according to the ascribed plant practices. All tests used a 2.2L self-aerated Denver flotation cell with an agitation of 1200 rpm.



# **5 Quantification of Adsorbed Reagents: Xanthate**

## **5.1 Abstract**

Quantitative analysis of collectors adsorbed onto mineral surfaces using Headspace Analysis Gas-phase Infrared Spectroscopy (HAGIS) is explored for the galena/xanthate system. Four possible standards have been evaluated: Sodium isopropyl xanthate, Pb-isopropyl xanthate, galena (PbS) conditioned with sodium isopropyl xanthate, and a Pb-sulphide ore conditioned with sodium isopropyl xanthate. All gave linear calibrations. For practical use, ores as standards are suggested.

## **5.2 Introduction**

Collector interactions with mineral surfaces have been the focus of many studies. Little work, however, has been done on direct quantification of the amount of collector adsorbed, especially in the industrial process. The use of Time-of-Flight Secondary Ion Mass Spectrometry (ToF-SIMS) has shown good characterization of individual particle coverage<sup>11-13</sup> but a large number of particles need to be analyzed to obtain acceptable reproducibility, which is time consuming and costly.

## **Chapter 5 – Quantification of Adsorbed Xanthate**

---

Studies using thermal decomposition of adsorbed collector as part of the analytical procedure such as differential thermal analysis<sup>8</sup> and selective oxidation<sup>9,10</sup> give good reproducibility. There is some concern, however, that the techniques rely on carbon species analysis, as it is known that carbon will be present at any particle surface (e.g., from CO<sub>2</sub> present in the air or in aqueous solution).

The technique used here takes advantage of thermal decomposition and uses infrared spectroscopy to identify and quantify the decomposition products. For instance, amines and xanthates produce distinctive peaks<sup>67</sup> (and, in principle, could be analyzed simultaneously). The technique is known as Headspace Analysis Gas-Phase Infrared Spectroscopy or HAGIS<sup>7</sup>.

As the first test system for the proposed technique, xanthate adsorption onto Pb sulphides was selected. This system is relatively simple in terms of interaction products (e.g., no dixanthogen formation)<sup>70</sup>. A calibration curve reporting adsorbed xanthate versus HAGIS peak area (inverse Beer's Law plot) is required to perform quantitative analysis. In order to prepare a calibration curve, a peak respective to adsorbed xanthate and dependent on concentration is selected. Vreughdenhil et al. reported that xanthates and metal xanthates decompose into CO, CO<sub>2</sub>, COS, CS<sub>2</sub> and ROH upon heating<sup>59</sup>. In metal xanthates, they observed that the relative intensity of each peak is dependent on the metal ion present. This may be an important point in choosing a standard system. In xanthate flotation of nickel oxides, Naklicki et al. observed an increased signal with increasing concentration<sup>71</sup>, a hint at its intended use here.

The xanthate tested is sodium isopropyl xanthate. Four possible standards are explored:

- a) Sodium isopropyl xanthate (the simplest possibility).
- b) A synthetic Pb-isopropyl xanthate (the likely interaction product).

## **Chapter 5 – Quantification of Adsorbed Xanthate**

---

- c) Galena (PbS) conditioned with sodium isopropyl xanthate in aqueous solutions (i.e., making no assumptions on surface species).
- d) A Pb-sulphide ore conditioned with sodium isopropyl xanthate as in batch flotation (i.e., closest to eventual use).

Mass balancing across the products of batch flotation of an ore is used to determine which calibration procedure is best, by summing the mass of xanthate detected on the products and comparing with the known amount added.

### **5.3 Procedure**

#### **5.3.1 Calibration**

##### **(a) Sodium Isopropyl Xanthate**

Sodium isopropyl xanthate (NaIPX, Charles Tenant Co. Ltd.) was dissolved in acetone and precipitated into petroleum ether for purification. The sample was dried and kept in a sealed container.

##### **(b) Pb-isopropyl Xanthate**

Pb(IPX)<sub>2</sub> was synthesized by slowly adding aqueous sodium isopropyl xanthate (Charles Tenant Co. Ltd., precipitated into petroleum ether from acetone and dried prior to use) to aqueous PbCl<sub>2</sub>. The light yellow precipitate was washed three times with diethyl ether (Fisher).

##### **(c) Galena**

A galena sample (Ward's Natural Science) was pulverized, screened to obtain a 53-75 μm size fraction and kept in a freezer to reduce oxidation. A stock solution (1x10<sup>-3</sup> M) of isopropyl xanthate (IPX) was prepared using pH 9 water (NaOH). The following concentrations were prepared from the stock solution: 1x10<sup>-5</sup>, 3x10<sup>-5</sup>, and 1x10<sup>-4</sup> M with pH 9 water. An aliquot of the IPX solutions was kept for calibration of the UV-Vis technique.

## **Chapter 5 – Quantification of Adsorbed Xanthate**

---

The galena samples (5g each) were conditioned with 100 mL IPX solutions ranging from 0 to  $1 \times 10^{-4}$  M on an orbital shaker (400 rpm) for 15 minutes. The pH was not adjusted after contact with galena.

The samples were filtered to near dryness on a Büchner funnel with a fritted glass disk of medium or fine porosity. The filtrates were analyzed by UV-Vis for indirect determination of IPX adsorption. The mg IPX adsorbed per gram mineral was calculated as the difference between the initial and final solution concentrations. After filtration, each sample was removed from the funnel and placed between two filter papers. The samples were left to air dry for approximately 30 minutes and the HAGIS spectra obtained.

### **(d) Brunswick Mine Ore**

A 500g sample of ore from Brunswick Mine (-10 mesh) was treated as per their typical batch flotation protocol. It was ground with 1.0g soda ash for 15 minutes at 67% solids in a stainless steel laboratory rod mill (100% mild steel rods) to obtain 72-75% passing 400 mesh. The slurry was transferred to a 1L Denver flotation cell (1200 rpm), the pH adjusted to pH 9.2, and the pulp aerated for 20 minutes.

After aeration, the pH was re-adjusted to 9.2, a known mass of xanthate and 3 drops MIBC were added and the slurry conditioned for 7 minutes. The solids were pressure filtered, the filtrate volume and UV-Vis spectrum obtained to determine IPX adsorption indirectly. The solids were set to dry between two sheets of KRAFT (brown) paper. Once sufficiently dry, the sample was rolled and mixed to obtain a representative sample and HAGIS spectra were obtained.

### **5.3.2 Analysis**

#### **(a) HAGIS**

The HAGIS spectrum for each sample was collected as follows:

## Chapter 5 – Quantification of Adsorbed Xanthate

- a. A sample was placed in the cell and the cell was purged with nitrogen (3 psi / 20.7 kPa) for 30 seconds and sealed.
- b. A background spectrum of the loaded cell was acquired (500 scans).
- c. The sample boat was heated to 190°C for a set time.
- d. The sample spectrum was acquired (500 scans).
- e. The peak areas were integrated according to Figure 5-1 (no corrections were performed).
- f. Once completely cooled, the sample masses were recorded.

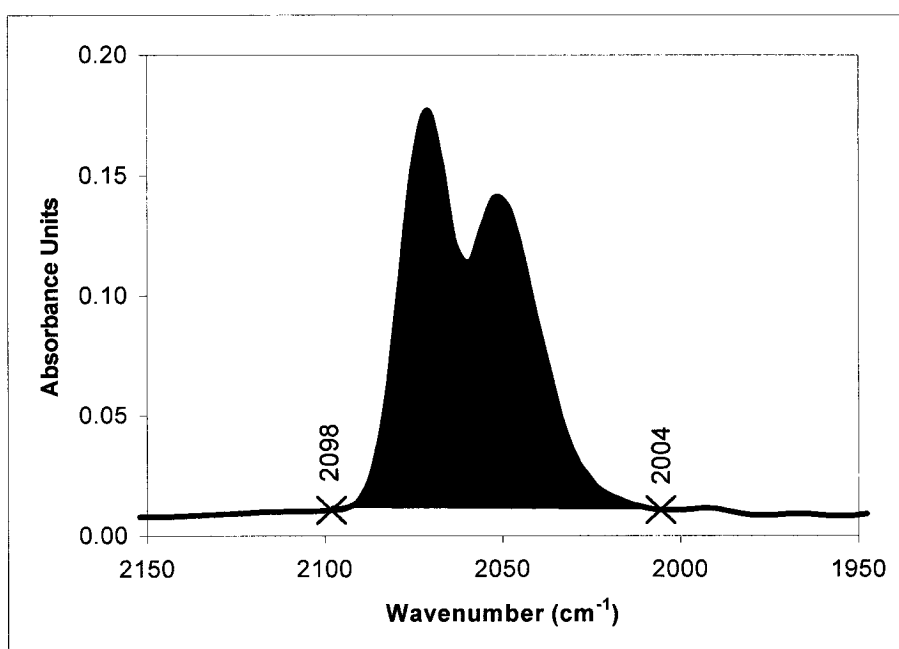


Figure 5-1 HAGIS Peak integration scheme for xanthate.

### (b) UV-Visible

A Milton Roy Spectronic 1201 UV-Visible spectrometer was used to determine the residual xanthate in the filtrates. Standard sodium isopropyl xanthate concentration was plotted versus the area under the characteristic xanthate peak (301 nm) to create a calibration curve. The amount of adsorbed xanthate was

## **Chapter 5 – Quantification of Adsorbed Xanthate**

---

determined indirectly by subtracting the residual xanthate from the known initial concentration.

### **5.3.3 Flotation**

The same conditioning protocol described in 4.3.1(d) was employed, except concentrate was collected for 7 minutes. Both products (concentrate and tails) were pressure filtered, and the filtrate volume and UV-Vis spectrum obtained to determine IPX adsorption indirectly. The solids were set to dry between two sheets of KRAFT (brown) paper. Once sufficiently dry, the sample was prepared to obtain a representative sample (rolled and mixed) and a minimum of three HAGIS spectra were taken of each product.

## **5.4 Results**

### **5.4.1 Comparison of HAGIS spectra**

The HAGIS spectra for the four systems are presented in Figure 5-2. The xanthate decomposition peaks are shown and are compared in Table 5-1. In the case of the ore, there is an additional peak at  $1250\text{ cm}^{-1}$  respective of  $\text{SO}_2$ . Although this peak does not interfere with the xanthate-related peaks, the result suggests there are ‘matrix’ effects that need to be considered.

## Chapter 5 – Quantification of Adsorbed Xanthate

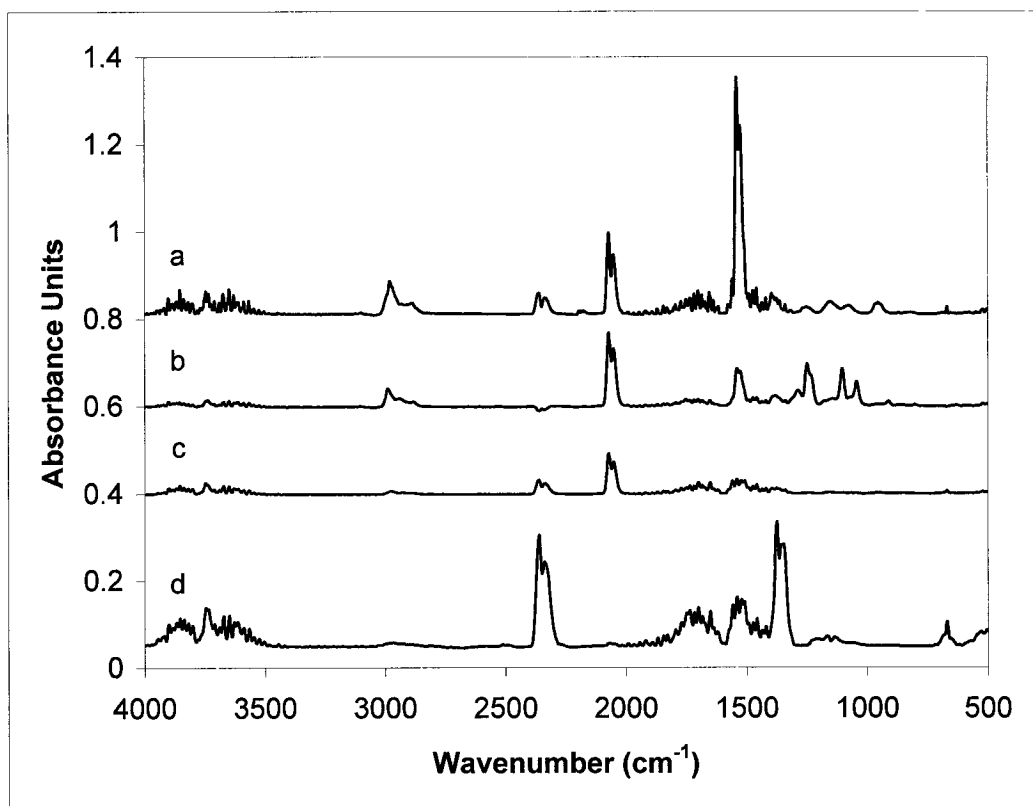


Figure 5-2 HAGIS spectra for (a) NaIPX, (b) Pb(IPX)<sub>2</sub>, (c) galena + IPX, and (d) Brunswick Mine ore + IPX.

Table 5-1 Xanthate decomposition peak positions and peak areas (% contribution to total for these four peaks)

Sample	CO (2180 cm <sup>-1</sup> )	CO <sub>2</sub> (2350 cm <sup>-1</sup> )	COS (2060 cm <sup>-1</sup> )	CS <sub>2</sub> (1535 cm <sup>-1</sup> )
NaIPX	1	9	24	66
Pb(IPX) <sub>2</sub>	0	0	68	32
Galena + IPX	0	42	20	37
Brunswick + IPX	0	80	2	18

The lack of CO<sub>2</sub> from Pb(IPX)<sub>2</sub> indicates this is not a consistent decomposition product of xanthate: the source in the other cases is largely environmental. The peak selected for calibration purposes is COS.

## Chapter 5 – Quantification of Adsorbed Xanthate

### 5.4.2 Calibration

In order to obtain calibration curves, the mass of xanthate contained in the sample (weighed in cases (a), (b) or measured indirectly by UV-Visible in cases (c), (d)) was plotted against the COS peak area. Linear calibration curves were obtained for all cases, sodium isopropyl xanthate (Figure 5-3a),  $\text{Pb}(\text{IPX})_2$  (Figure 5-3b), xanthate adsorbed on galena (Figure 5-4), and xanthate adsorbed on Brunswick Mine ore (Figure 5-5). Each standard curve was then tested against the Brunswick Mine batch flotation products (Table 5-2). In the case of sodium isopropyl xanthate, the mass of adsorbed xanthate calculated using the linear regression is lower than that estimated indirectly. This may be a result of desorption kinetics. The chemical bond that needs to be broken is much stronger in the case of the adsorbed xanthate (S – Pb rather than S – Na).

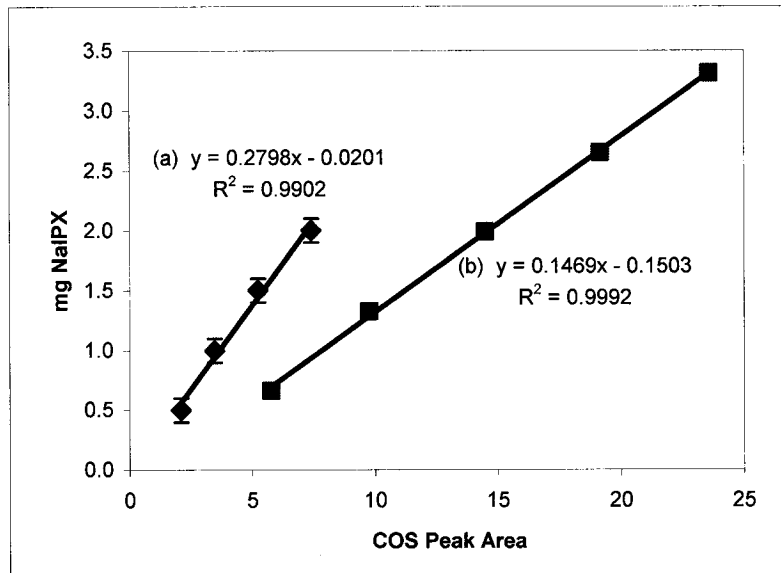


Figure 5-3 HAGIS calibration curve for sodium isopropyl xanthate (NaIPX) (a) pure and (b) derived from  $\text{Pb}(\text{IPX})_2$ .



## Chapter 5 – Quantification of Adsorbed Xanthate

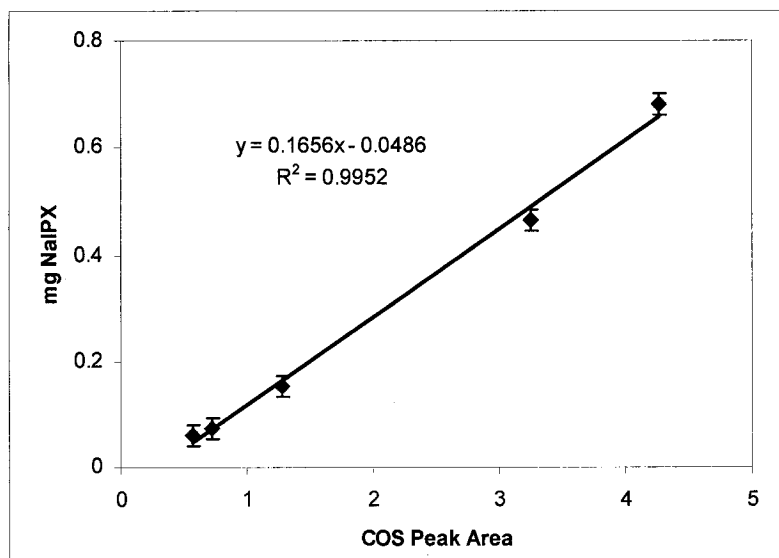


Figure 5-4 HAGIS calibration curve for IPX adsorbed onto galena. (mg IPX determined by difference using UV/Vis analysis on solutions)

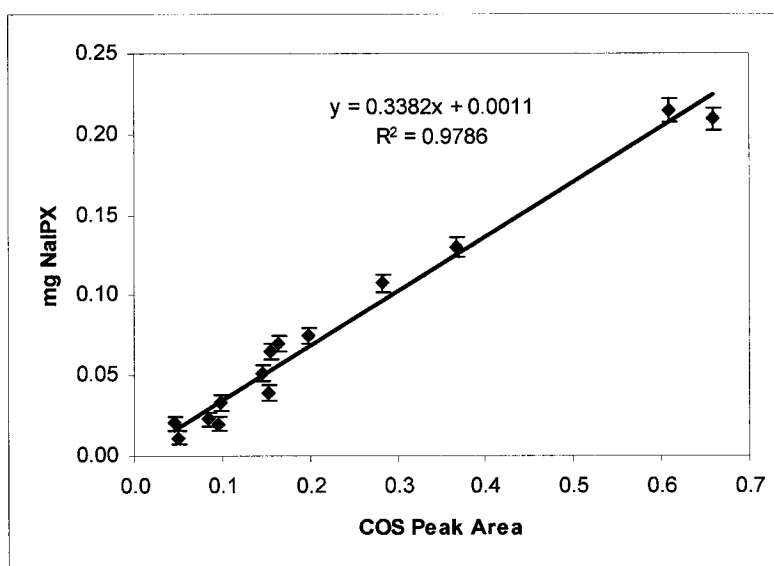


Figure 5-5 HAGIS calibration curve for IPX adsorbed onto Brunswick Mine ore. Data points are a combination of changing IPX mass and sample mass.

For the  $\text{Pb}(\text{IPX})_2$  and galena standards (the curve was forced through zero to avoid negative values), xanthate adsorption was underestimated by about half. Underestimation most likely occurs because thermal decomposition of pure  $\text{Pb}(\text{IPX})_2$  takes place more readily than the desorption/decomposition of adsorbed

## Chapter 5 – Quantification of Adsorbed Xanthate

species, resulting in a smaller slope in the calibration plot. It may also imply that xanthate desorption is not complete for the samples from batch flotation. Another aspect is the protocol. In the case of galena, the standards were simply filtered and not allowed to dry completely while the batch flotation products were left to dry for 24-48 hours.

Using the Brunswick Mine ore for calibration avoids many of these issues. The result was an excellent mass balance (Table 5-2). The verification of the mass balance establishes the proposed quantification technique, and indicates that ores should be used as standards. The relative ease of sample preparation is preserved and possible matrix effects allowed for. It also means the protocol for standard preparation is more readily matched to that of the sample compared to the other possible calibration approaches tried.

Table 5-2 Comparison of calibration procedures for the determination of IPX adsorption onto Brunswick Mine ore flotation products (reported as mg).

Sample	IPX added	UV-Vis *	NaIPX	Pb(IPX) <sub>2</sub>	Galena	Ore
#1 Conc.			9.4	4.7	5.1	11.1 ± 1.8
#1 Tail			5.7	2.8	3.1	7.3 ± 0.5
#1 Total	20.0	19.3	15.1	7.6	8.2	18.4 ± 1.9
#2 Conc.			9.3	4.6	5.0	12.4 ± 1.4
#2 Tail			12.5	6.3	6.8	16.2 ± 0.9
#2 Total	30.0	28.4	21.8	10.9	11.8	28.6 ± 1.7

\* IPX adsorption calculated indirectly (initial mg IPX – mg IPX remaining in solution)

The matrix effect likely to be encountered is the relative ease of thermal desorption of the adsorbed xanthate. Comparing the ore to galena, the ore contains several other minerals with which xanthate may interact. In these cases, the rate of thermal desorption might not be the same for all components. This might suggest a discrepancy could be incurred between the concentrate and tail samples, that the same calibration would not apply to both. There was no

## **Chapter 5 – Quantification of Adsorbed Xanthate**

evidence of this with the Brunswick Mine ore. In some cases calibration may have to be specific for the product, concentrate vs. tail.

The technique gives us information about the distribution of collector between the products, not readily available by other methods. Comparing the two batch flotation tests, note that when xanthate dosage is increased, there is a significant increase (250%) in xanthate reporting to tails and no increase in the xanthate on the concentrate (the mg/g column in Table 5-3).

Table 5-3 Xanthate adsorption levels (mg/g) on Brunswick Mine batch flotation products (Ore calibration)

Sample	Mass (g)	Mass HAGIS (g)	COS Area	Mass NaIPX (mg)	mg/g	Total mg
#1 Conc.	113.59	0.42	0.13	0.044	0.10	11.7 ± 1.6
#1 Tail	394.74	1.71	0.09	0.033	0.02	7.6 ± 1.3
#1 Total	506.70					19.3 ± 3.1
#2 Conc.	132.18	0.37	0.10	0.034	0.09	12.1 ± 2.0
#2 Tail	358.00	0.61	0.08	0.028	0.05	16.5 ± 3.1
#2 Total	491.00					28.6 ± 5.1

### **5.4.3 Effect of Heating Time and Temperature**

The results obtained with all four standards point to the fact that the protocol needs to be followed strictly. The effects of heating time and temperature on the COS peak area obtained for a metal xanthate are shown in Figure 5-6. In this case, the peak area increases with heating time to reach a plateau at 120 minutes. The linear calibration curves obtained for all four systems, that when heating time and temperature are kept the same, indicate that the protocol employing the COS peak is appropriate for quantitative analysis.

## Chapter 5 – Quantification of Adsorbed Xanthate

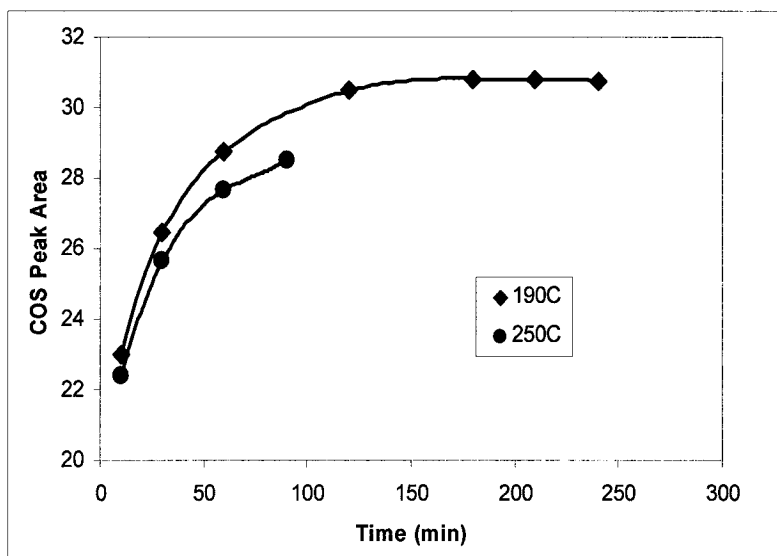


Figure 5-6 Effect of heating time on COS peak area at two temperatures: 190°C and 250°C.

### 5.5 Discussion

Although linear calibration curves were observed for all systems, the use of ore as standard was the only one to give an accurate result for the mass balance. The initial hope was for a “universal” standard based on xanthate or some simple derivatives (metal xanthate, mineral/xanthate interaction products). This is not the situation, as a mass balance was not achieved using any of these standards. In the case of Pb-xanthate, the low results are attributed to the different rate of desorption/decomposition. The Pb-xanthate adsorbed at the mineral surface has a slower desorption rate than the pure Pb-xanthate compound due to the strong surface bond. There is also a question of heat transfer. In the case of Pb-xanthate, heat is directly applied to the compound; when adsorbed on a mineral surface, much of the heat is transferred to the mineral.

In the case of galena, the HAGIS spectra were obtained after little or no drying of the mineral, a conveniently simple routine. Drying of the samples appears to have an impact on the level of desorption. This implies that either some xanthate is lost

## **Chapter 5 – Quantification of Adsorbed Xanthate**

---

to the atmosphere (evaporation from exposure to light) or that adsorption of atmospheric gases could retard desorption or alter the desorption products. While it may be possible to devise a suitable calibration using these simple xanthate products, the use of ore as standard avoids the issues. As demonstrated, it produces an accurate mass balance, in part because the protocols are readily made the same for the calibration as well as the test samples.

The successful mass balance introduces the use of the HAGIS technique as a quantitative analysis tool for adsorbed collectors in mineral processing. With modifications to the current cell such as increasing the size of the sample boat, it may be used to monitor any organic reagent adsorbed on ores and processing products that desorbs/decomposes under reasonable temperatures (<300°C) and times. Applications in plant operations range from incorporating into control strategies to environmental accounting of reagents.

### **5.6 Conclusions**

1. HAGIS is introduced as a tool to quantify adsorbed collector under flotation conditions.
2. Linear calibrations were obtained for xanthate, metal-xanthate and adsorbed products on galena and ores.
3. Mass balancing the amount of adsorbed xanthate on batch flotation samples indicated the ore/xanthate system was the best choice for calibration.
4. HAGIS shows promise for a variety of adsorbed organic compounds encountered in mineral processing (and elsewhere).

# **6 Quantification of Adsorbed Reagents: Amines**

### **6.1 Abstract**

The use of Headspace Analysis Gas-Phase Infrared Spectroscopy (HAGIS) is tested for quantitative determination of adsorbed amines. Two collectors, dodecylamine and diphenylguanidine and a depressant, triethylenetetramine, were studied. A peak at  $1032\text{ cm}^{-1}$ , corresponding to the R – NH<sub>x</sub> functional group of a thermally desorbed product, was used to prepare calibrations. The test case, diphenylguanidine adsorbed on Inco matte, showed that the HAGIS technique could be used to quantify adsorbed amines.

### **6.2 Introduction**

Reagent interaction with mineral surfaces is the basis of the flotation process. It is clear that the direct quantification of the amount of collector adsorbed, especially in the industrial process, would be an asset to research and to operations. Techniques such as Time-of-Flight Secondary Ion Mass Spectrometry (ToF-SIMS) are able to characterize individual particle coverage<sup>11-13</sup> but only relative quantification is possible.

## Chapter 6 – Quantification of Adsorbed Amines

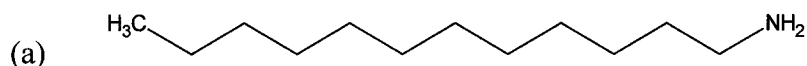
---

Howe and Pope<sup>8</sup> have reported the quantitative determination of dodecylamine and sodium oleate on titanium dioxide using differential thermal analysis. Similarly, Pugh and Husby<sup>9</sup> quantified the adsorption of dodecylamine, sodium oleate and xanthate by detecting evolved carbon dioxide upon selective oxidation of the mineral surface. Miettinen et al.<sup>10</sup> also used a combustion technique to determine the amount of sarcosine-type collector adsorbed onto phosphate ores. These techniques all show the ability to detect collectors at levels used in industry.

The aim of this chapter is to explore the use of Headspace Analysis Gas-Phase Infrared Spectroscopy (HAGIS)<sup>7</sup> in quantifying adsorbed amines. The technique takes advantage of thermal decomposition/desorption and uses infrared spectroscopy to identify and quantify the decomposition products. The work with a xanthate/galena system (Chapter 5) produced good quantification results<sup>72</sup>. As a second exercise, amine-type reagents are considered: two collectors, dodecylamine (DDA – Figure 6-1a) and diphenylguanidine (DPG – Figure 6-1b), and a depressant, triethylenetetramine (TETA – Figure 6-1c).

Dodecylamine is used in flotation in the form of *unsubstituted salts* such as acetate,  $C_{12}NH_3^+CH_3COO^-$ , or hydrochloride,  $C_{12}NH_3^+Cl^-$ . It is the most common reagent for the flotation of silicate minerals<sup>68</sup>.

Both DPG and TETA are chelating-type reagents, i.e., they will form coordination bonds with metal ions. Diphenylguanidine is used as collector/frother in the processing of Inco Bessemer matte. The process includes selective flotation of the copper mineral (chalcocite, Cc,  $Cu_2S$ ) from the nickel mineral (heazlewoodite, Hz,  $Ni_3S_2$ ) using DPG<sup>73</sup>.



## Chapter 6 – Quantification of Adsorbed Amines

---

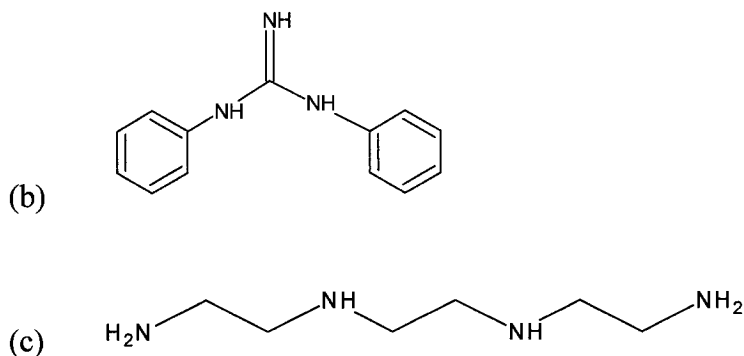


Figure 6-1 Schematic diagram for (a) dodecylamine, (b) diphenylguanidine and (c) triethylenetetramine.

Triethylenetetramine is used to depress hexagonal pyrrhotite (non-magnetic) in similar fashion to DETA (diethylenetriamine)<sup>4</sup>. At least part of the mechanism of pyrrhotite depression for both DETA and TETA appears to be the removal of heavy metal ions (notably potential activators – Cu, Ni, Co) from the surface of the pyrrhotite<sup>4,74,75</sup>. This cleaning action reduces the number of active sites for collector adsorption on the pyrrhotite and effectively depresses it.

The protocol for quantitative HAGIS has been determined in Chapter 5. The following steps are followed here:

1. Identification of the desorption products. The key is to find peaks that belong to the desorption product and are dependent on concentration.
2. Preparation of a calibration curve, concentration vs. peak area, preferably using reagents adsorbed onto ores as standards.
3. Test the calibration on batch flotation products. By performing a mass balance of total adsorbed reagent on concentrate and tail samples, calibration can be validated.



## **Chapter 6 – Quantification of Adsorbed Amines**

---

### **6.3 Experimental**

#### **6.3.1 Reagents**

Diphenylguanidine (Acros Organics) was used as received and added in powder form. Stock solutions were prepared for dodecylamine ( $2.5 \times 10^{-4}\text{M}$ , Eastman Kodak), triethylenetetramine (1.0 g/L, Aldrich) and sodium sulphite (4.0 g/L, Fisher Scientific Co.).

#### **6.3.2 Diphenylguanidine Adsorption on Inco Matte**

A bulk matte sample from Inco Technical Services Limited (ITSL), was used as received for batch flotation tests. The batch flotation procedure was based on ITSL practice<sup>76</sup>. A 1 kg bulk matte sample was ground in a laboratory stainless steel rod mill with a mixture of mild and stainless steel rods for 10 minutes at 75 w/w % solids at pH 12 (lime). The solids were transferred to a 3 L Denver flotation cell and agitated at 1200 rpm and magnetic separation was performed using a hand magnet for 10 minutes. The solids were allowed to settle and returned to the rod mill (with minimal pH 12 water addition) with addition of DPG and ground for 6 minutes. In the final step, the slurry was transferred to the 3 L cell with pH 12 water and concentrate recovered until the froth was barren (~ 4 minutes). No frother addition was required. The samples were pressure filtered and dried between two sheets of KRAFT (brown) paper. In the case of preparing standards, the flotation step was omitted.

#### **6.3.3 Triethylenetetramine Adsorption on Voisey's Bay Nickel Co. Ore**

Voisey's Bay ore samples were pulverized to 100% -150  $\mu\text{m}$ . Samples were conditioned on an orbital shaker with 100g/t TETA and 400g/t sodium sulphite for 30 minutes at pH 9.5. The slurry was filtered and the solids rinsed 3 times with 100mL water at pH 9.5. The slurry was filtered once more. A sample of the initial solution and all filtrates were analyzed for TETA content using LC-MS (MAXXAM Analytics Inc.). The solids were air dried and examined for the presence of TETA using HAGIS.

## **Chapter 6 – Quantification of Adsorbed Amines**

---

### **6.3.4 Dodecylamine Adsorption on Quartz**

A quartz sample was pulverized and screened to the following sizes: 212-300, 300-425, and 425-800  $\mu\text{m}$ . All three samples were conditioned with a dosage of 0.55 mg/g (100 mL stock solution for 10 g quartz) dodecylamine at pH 10 (NaOH). The samples were filtered, washed and dried in air for a minimum of 24 hours. Once dried, the samples were stored in a sealed bottle in a freezer.

### **6.3.5 HAGIS**

The HAGIS spectrum for each sample was collected as follows:

- a. A sample was placed in the boat and the cell was purged with nitrogen (3 psi / 20.7 kPa) for 30 seconds and sealed.
- b. A background spectrum of the loaded cell was acquired (500 scans) with a Bruker IFS-66 infrared spectrometer and a nitrogen cooled MCT detector.
- c. The sample boat was heated to 250-290°C for a set time (indicated in each case).
- d. The sample spectrum was acquired (500 scans).
- e. The peak areas were integrated according to Figure 6-2 (no corrections were performed).
- f. Once completely cooled, the sample masses were recorded.

### **6.3.6 UV-Visible**

A Milton Roy Spectronic 1201 UV-Visible spectrometer was used to determine the residual diphenylguanidine in the filtrates. Standard DPG concentration was plotted versus the area under the characteristic DPG peak at pH > 11 (254 nm) to create a calibration curve. The amount of adsorbed DPG was determined indirectly by subtracting the residual from the known initial concentration.

## Chapter 6 – Quantification of Adsorbed Amines

---

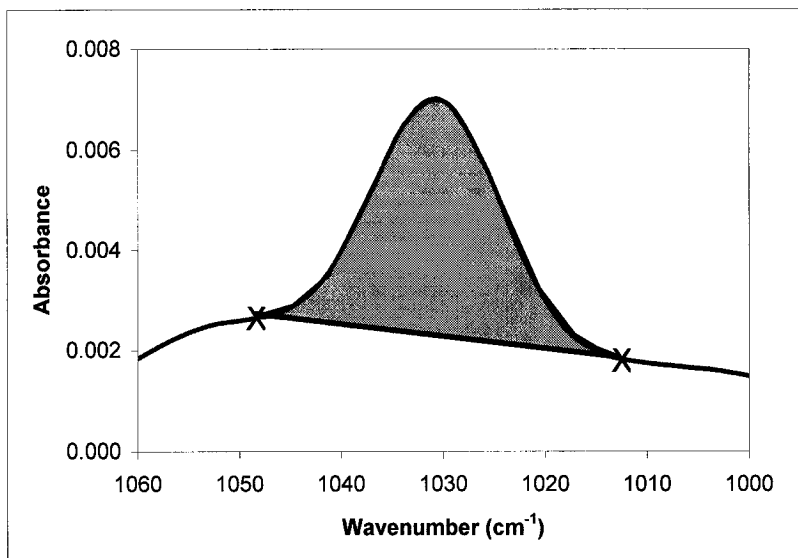


Figure 6-2 HAGIS peak integration scheme for amines.

### 6.4 Results

#### 6.4.1 Identification of Peaks

The HAGIS spectra for the three systems are presented in Figure 6-3. There is a peak common to all at  $1032\text{ cm}^{-1}$ . According to the vapour spectra data in Table 6-1, this peak is due to the deformation ( $\delta(\text{NH})$ ) vibrational mode for primary aliphatic amines.

## Chapter 6 – Quantification of Adsorbed Amines

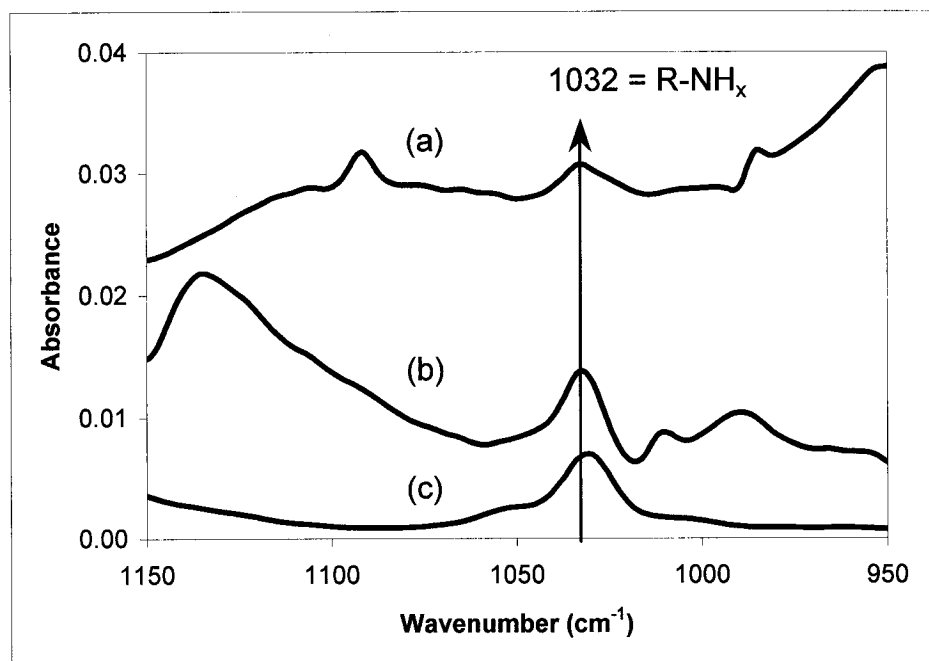


Figure 6-3 HAGIS spectra for the desorption products of (a) dodecylamine on quartz (300°C, 10 min), (b) triethylenetetramine on Voisey's Bay Nickel Co. ore (290°C, 10 min), (c) diphenylguanidine on Inco matte (250°C, 5 min).

Table 6-1 Band Maxima in the Infrared Vapour Phase Spectra of Amines in the 1250 to 700  $\text{cm}^{-1}$  range.<sup>77</sup>

Vibrational Mode	Compound	Frequency ( $\text{cm}^{-1}$ )
Deformation, $\delta(\text{NH})$ including some stretching, $\nu(\text{C-N})$	Primary aliphatic, normal	1090-1070 (w)
	Primary aliphatic, $\alpha$ -branched	1160-1145 (ms)
		1070-1010 (w)
	Secondary aliphatic	1155-1135 (s)
		1025-1015 (w) 905-875 or 965-930 (w)
Bending, $\beta(\text{NH})$	Primary aliphatic	790-765 (s)
	Secondary aliphatic	725-710 (s)

\* For aromatic amines, the band maxima are generally at higher frequencies than observed for aliphatic amines.

## Chapter 6 – Quantification of Adsorbed Amines

### 6.4.2 Calibration Curve – DPG on Inco Matte

Three standard concentrations of DPG adsorbed on Inco matte were used to prepare a calibration curve by varying sample mass (Figure 6-4). The amount of DPG adsorbed for each standard was determined by UV-Visible spectroscopy (difference between initial amount added and amount remaining in solution). This was divided by the total sample mass to give the standard concentration (mg/g). The amount of DPG present in the HAGIS cell is then determined by multiplying the mass of sample inserted in the cell by the standard concentration. The calibration curve represents mass of DPG versus the peak area at  $1032\text{ cm}^{-1}$ .

The assignment of the calibration peak ( $1032\text{ cm}^{-1}$ ) as an  $\text{R} - \text{NH}_x$  peak signifies it may be possible to use the DPG calibration curve for all reagents that have primary amines as desorption products. The simple translation of mass of DPG into moles of  $\text{R} - \text{NH}_x$  produces a “universal” calibration curve Figure 6-5. The number of  $\text{R} - \text{NH}_x$  groups are, as observed in Figure 6-1: DDA = 1, DPG = 2, and TETA = 4.

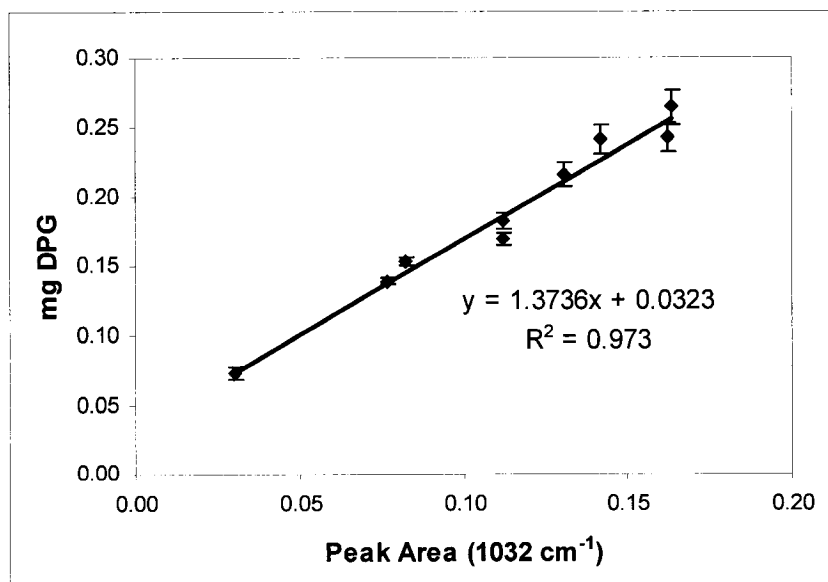


Figure 6-4 HAGIS calibration curve for DPG adsorbed onto Inco matte (mg DPG determined by difference using UV/Vis analysis on solutions) (all samples at  $250^\circ\text{C}$ , 5 min).

## Chapter 6 – Quantification of Adsorbed Amines

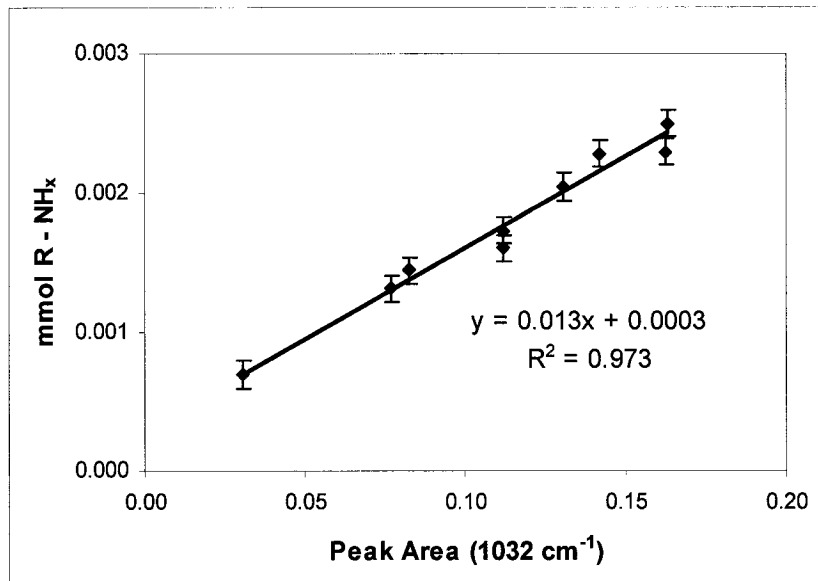


Figure 6-5 “Universal” HAGIS calibration curve for amines (derived from DPG on Inco matte).

### 6.4.3 Mass Balance

Preliminary results of DPG quantification on Inco matte batch flotation products show that a close mass balance is achieved for sample #2 (Table 6-2). In all three cases, a large error is imparted due to the tail (a small error in adsorption levels results in a large error in the total due to the high mass).

Table 6-2 Mass balance for DPG adsorbed on Inco Matte

Sample	Added DPG (mg)	Adsorbed DPG (mg) by UV-Vis	Product Mass (g)	Adsorbed DPG (mg/g)	Adsorbed DPG (mg) by HAGIS
#1 Conc.			98.74	0.06	5.9 ± 0.9
#1 Tail			278.71	0.07	20.5 ± 2.8
#1 Total	25.1	17.5	377.45		26.4 ± 2.9
#2 Conc.			133.70	0.10	10.8 ± 1.3
#2 Tail			249.94	0.03	8.0 ± 2.0
#2 Total	37.5	19.1	383.64		18.8 ± 2.5

## Chapter 6 – Quantification of Adsorbed Amines

#3 Conc.			113.66	0.12	16.5 ± 1.8
#3 Tail			286.79	0.05	12.0 ± 1.8
#3 Total	50.1	23.5	400.45		28.5 ± 2.6

For triethylenetetramine, using the DPG on Inco matte calibration curve, a relatively good mass balance of TETA adsorption on Voisey's Bay Nickel Co. ore was produced (Table 6-3). The results fall within the standard error but are all underestimated.

Table 6-3 Mass balance of TETA adsorbed on Voisey's Bay Nickel Co. ore.

Sample	Adsorbed TETA (mg) by LC-MS	mmol NH	Adsorbed TETA (mg/g)	Adsorbed TETA (mg) by HAGIS
#1	49.7	0.0015	0.8812	44.1 ± 5
#2	40.3	0.0018	1.0295	35.9 ± 5
#3	54.3	0.0012	0.7177	51.5 ± 5

The same calibration was also used to determine the adsorption of dodecylamine on quartz (Table 6-4). It is observed that the adsorption level increases with decreasing particle size (increasing surface area). The level of adsorption is comparable to that reported by Pugh and Husby<sup>9</sup>. Lack of a convenient indirect analysis procedure prevents completing the mass balance.

Table 6-4 Dodecylamine adsorption on quartz.

Sample size (µm)	Dosage DDA (M)	Sample mass to HAGIS (g)	mmol NH = mmol DDA	Adsorbed DDA (x 10 <sup>-6</sup> mol/g)
212-300	5.0 x 10 <sup>-4</sup>	1.0	0.0016	1.6 ± 0.2
300-425	5.0 x 10 <sup>-4</sup>	0.5	0.0007	0.7 ± 0.1
425-800	5.0 x 10 <sup>-4</sup>	0.5	0.0007	0.7 ± 0.1
200-800 <sup>9</sup>	1.2 x 10 <sup>-4</sup>			0.479

## **Chapter 6 – Quantification of Adsorbed Amines**

---

### **6.5 Discussion**

The identification of desorption products proved easy when comparing similar reagents; the characteristic peak quickly became apparent. It is important to take into account the molecular structure and the adsorption mechanism of the reagent in question when trying to determine the thermal desorption / decomposition products.

The calibration curve observed in the case of DPG on Inco matte shows some scatter. This is likely due to the low absorbance values obtained. Beer's law is usually recommended to an absorbance of 1; at the low concentrations here, the maximum absorbance for the peak at  $1032\text{ cm}^{-1}$  is approximately 0.005.

Representing the DPG data in terms of mol R – NH<sub>x</sub> opens new opportunities; one can now directly quantify the adsorption of reagents that are typically not readily quantifiable, even indirectly (e.g., dodecylamine). In the case of TETA, a bias (underestimation) was observed. At present, this bias is attributed to protocol differences between experiments (e.g., the procedure was not the same for filtering and drying of the samples and, more importantly, the heating temperature and time were different).

The exercise with amines again shows that the HAGIS technique is a promising tool for the quantitative determination of adsorbed reagents. Further testing and the development of protocols for in-plant testing is warranted.

### **6.6 Conclusions**

The following conclusions can be drawn:

1. Adsorbed amines have a characteristic thermal desorption peak at  $1032\text{ cm}^{-1}$ .



## **Chapter 6 – Quantification of Adsorbed Amines**

---

2. The argument is advanced that only one standard system is needed to prepare a “universal” amine calibration curve.
3. Quantification appears feasible.

# **7 Conclusions**

The following overall conclusions are reached:

1. Quantitative analysis using the HAGIS technique is possible.
2. A protocol has been established and must be followed.
3. It is recommended to use reagents adsorbed on ores as calibration standards.
4. The use of infrared spectroscopy opens the technique to a variety of collectors and other organic reagents.

### **7.1 Protocol for the Quantification of Adsorbed Reagents using HAGIS**

The following protocol has been determined for the quantification of all adsorbed reagents:

1. The reagent is adsorbed on a mineral or ore, in a manner as close to the industrial process as possible, filtered and dried between two sheets of opaque paper at room temperature.
2. The dried sample is inserted into the HAGIS, the cell purged with nitrogen for 30 seconds and sealed.

## Chapter 7 – Conclusions

---

3. The sample boat is heated to a temperature at least 20°C above the boiling point of the reagent and HAGIS spectra are taken every 10 minutes for 1 hour.
4. A thermal decomposition/desorption peak is identified for the reagent.
5. Standards are prepared using varying concentrations of reagent. Reagent adsorption is determined by an indirect method such as UV-Vis spectroscopy.
6. HAGIS temperature and heating time are selected from the results in 3.
7. The HAGIS spectra for varying masses of the standards are taken and the designated peak is integrated (Figure 7-1). The mass of reagent added to the cell is calculated from the mass and adsorption concentration of standard used. A calibration curve, mass of reagent vs. peak area, is produced.
8. Unknown samples are prepared following the procedure in item 1.
9. The HAGIS spectra are taken for multiple samples of the unknown and the peaks are integrated using the same HAGIS settings and integration scheme as the standards.

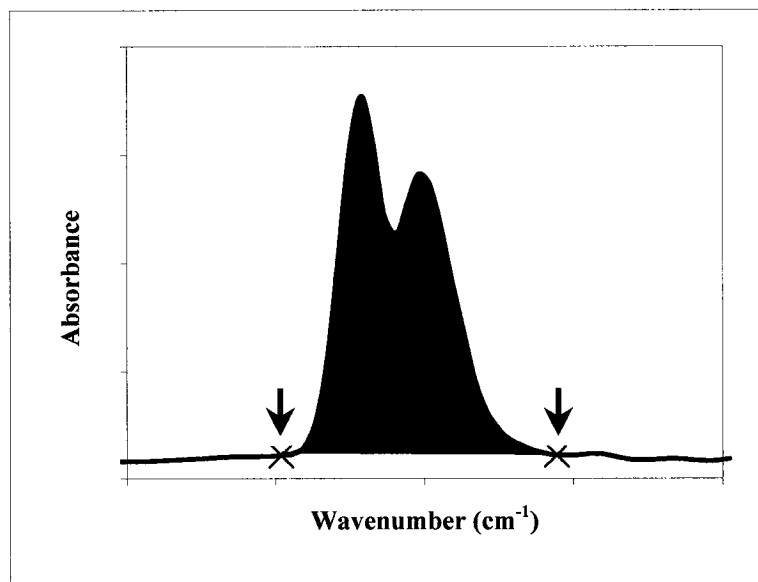


Figure 7-1 Example of the HAGIS peak integration scheme.

## **Chapter 7 – Conclusions**

---

### **7.2 Future Work**

There are many areas where further work could be conducted:

1. The use of ores as standards needs to be verified with ores of different composition. This may be done easily with the xanthate system.
2. The HAGIS technique may be employed to quantify the adsorption of mixed collector or mixed reagent systems.
3. A portable apparatus or an automated technique that could be part of the plant control system could be envisaged.

## References

---

# References

1. Gaudin, A.M., **1939**, Principles of Mineral Dressing, McGraw-Hill Book Company, Inc., New York, NY, p. 394.
2. Yoon, R.-H., Basilio, C.I., Marticorena, M.A., Kerr A.N., and Stratton-Crawley, R., **1995**, A Study of the Pyrrhotite Depression Mechanism by Diethylenetriamine, *Minerals Eng.*, Vol. 8, No. 7, 807-816.
3. Kelebek, S., Wells, P.F., and Fekete, S.O., **1996**, Differential Flotation of Chalcopyrite, Pentlandite and Pyrrhotite in Ni-Cu Sulphide Ores, *Can. Metall. Quart.*, Vol. 35, No. 4, 329-336.
4. Kelebek, S. and Tukel, C., **1999**, The Effect of Sodium Metabisulfite and Triethylenetetramine System on Pentlandite-Pyrrhotite Separation, *Int. J. Miner. Process.*, Vol. 57, 135-152.
5. Leja, J. and Schulman, J.H., **1954**, Flotation Theory: Molecular Interaction Between Frothers and Collector at Solid-Liquid-Air Interfaces, *Trans. AIME*, Vol. 16, 221-228.
6. Boulton, A., Fornasiero, D., and Ralston, J., **2003**, Characterisation of Sphalerite and Pyrite Flotation Samples by XPS and ToF-SIMS, *Int. J. Miner. Process.*, Vol. 70, Issues 1-4, , 205-219.
7. Vreugdenhil, A.J., Finch, J.A., Butler, I.S., and Paquin, I., **1999**, Analysis of Alkylxanthate Collectors on Sulphide Minerals and Flotation Products by Headspace Analysis Gas-Phase Infrared Spectroscopy (HAGIS), *Minerals Eng.*, Vol. 12, No. 7, 745-756.
8. Howe, T.M. and Pope, M.I., **1970/71**, The Quantitative Determination of Flotation Agents Adsorbed on Mineral Powders, Using Differential Thermal Analysis, *Powder Tech.*, Vol. 4, 338-344.
9. Pugh, R.J. and Husby, K., **1986**, Quantitative Determination of Collector Adsorbed on Fluorite, Galena and Quartz Particles by Selective Oxidation Surface Analysis, *Int. J. Min. Process.*, Vol. 18, 263-275.

## References

---

10. Miettinen, M., Stén, P., Bäckman, S., Leppinen, J., and Aaltonen, J., **2000**, Determination of Chemicals Bound to Mineral Surfaces in Flotation Processes, *Minerals Eng.*, Vol. 13, No. 3, 245-254.
11. Bolin, N.J., Chryssoulis, S.L., and Martin, C.J., **1997**, A Surface Study of a Boliden Ore by ToF-LIMS, *Int. J. Miner. Process.*, Vol. 51, 27-37.
12. Dimov, S.S. and Chryssoulis, S.L., **1998**, Standardization of Time-of-Flight Laser Ionization Mass Spectrometry Analysis of Minerals, *Spectrochim. Acta B*, Vol. 53, 399-406.
13. Piantadosi, C. and Smart, R.St.C., **2002**, Statistical Comparison of Hydrophobic and Hydrophilic Species on Galena and Pyrite Particles in Flotation Concentrate and Tails from ToF-SIMS Evidence, *Minerals Eng.*, Vol. 13, No. 13, 1377-1394.
14. Smith, B.C., **1996**, Fundamentals of Fourier Transform Infrared Spectroscopy, CRC Press, Boca Raton, FL, Chapter 5, 139-156.
15. Smith B.C., **2002**, Quantitative Spectroscopy: Theory and Practice, Academic Press, San Diego, Ca, 200 p.
16. Buckley, A. N., Woods, R., and Wouterlood, H. J. **1989**, An XPS Investigation of the Surface of Natural Sphalerites under Flotation-Related Conditions, *Int. J. Miner. Process.*, Vol. 26, 29-49.
17. Brienne, S. H. R., Zhang, Q., Butler, I. S., Xu, Z., and Finch, J. A. **1994**, X-ray Photoelectron and Infrared Spectroscopic Investigation of Sphalerite Activation with Iron, *Langmuir*, Vol. 10, 3582-3586.
18. Smart, R. St. C. **1991**, Surface Layers in Base Metal Sulphide Flotation, *Minerals Eng.*, Vol. 4, Nos. 7-11, 891-909.
19. Lascelles D., Sui, C. C., Finch, J. A., and Butler, I. S. **2001**, Copper Ion Mobility in Sphalerite Activation, *Colloids and Surfaces A: Physicochem. Eng. Aspects*, Vol. 186, 163-172.
20. Petrovykh, D.Y., Kimura-Suda, H., Whitman, L.J., and Tarlov, M.J., **2003**, Quantitative Analysis and Characterization of DNA Immobilized on Gold, *J. Am. Chem. Soc.*, Vol. 125, 5219-5226.
21. Allen, G.C., Eastman, J.R., Hallam, K.R., Graveling, G.J., Ragnarsdottir, K.V., and Skuse, D.R., **1999**, Mineral/Reagent Interactions: An X-ray Photoelectron Study of Adsorption of Reagents onto Mixtures of Minerals, *Clay Minerals*, Vol. 34, No. 1, 51-56.

## References

---

22. Clifford, R.K., Purdy, K.C., and Miller, J.D., **1975**, Characterization of Sulphide Mineral Surfaces in Froth Flotation Systems using Electron Spectroscopy for Chemical Analysis, *Amer. Inst. Chem. Eng. Symp. Ser.*, Vol. 71, 138-147.
23. Laajalehto, K., Kartio, I., and Suoninen, E. **1997**, XPS and SR-XPS Techniques Applied to Sulphide Mineral Surfaces, *Int. J. Miner. Process.*, Vol. 51, 163-170.
24. Szargan, R., Uhlig, I., Wittstock, G., and Roßbach, P, **1997**, New Methods in Flotation Research – Application of Synchrotron Radiation to Investigation of Adsorbates on Modified Galena Surfaces, *Int. J. Miner. Process.*, Vol. 51, 151-161.
25. Contini, G., Marabini, A.M., Di Castro, V., and Polzonetti, G., **1997**, 5-methyl-2-mercaptobenzoxazole Adsorbed on Cu<sub>2</sub>S Surface Studied by Synchrotron Radiation Excited Photoemission, *Int. J. Miner. Process.*, Vol. 51, 209-215.
26. Patrick, R. A. D., England, K. E. R., Charnock, J. M., Mosselmans, J. F. W., **1999**, Copper Activation of Sphalerite and its Reaction with Xanthate in Relation to Flotation: X-ray Absorption Spectroscopy (Reflection Extended X-ray Absorption Fine Structure) Investigation, *Int. J. Miner. Process.*, Vol. 55, 247-265.
27. O’Dea, A. R., Prince, K. E., Smart, R. St. C., and Gerson, A. R., **2001**, Secondary Ion Mass Spectrometry Investigation of the Interaction of Xanthate with Galena, *Int. J. Miner. Process.*, Vol. 61, 121-143.
28. Nagaraj, D.R. and Brinen, J.S., **1996**, SIMS and XPS Study of Adsorption of Sulfide Collectors on Pyroxene: A Case for Inadvertent Metal in Activation, *Colloids and Surfaces A: Physicochem. Eng. Aspects*, Vol. 116, 241-249.
29. Nagaraj, D.R. and Brinen, J.S., **2001**, SIMS Study of Adsorption of Collectors on Pyrite, *Int. J. Miner. Process.*, Vol. 63, 45-57.
30. Nägele, E., Schneider, U., **1985**, Analysis of Surfactants Adsorbed on Cement using Secondary Ion Mass Spectrometry (SIMS), *Cement and Concrete Research*, Vol. 15, 1022-1026.
31. Piantadosi, C., Jasieniak, M., Skinner, W. M., and Smart, R. St. C. **2000**, Statistical Comparison of Surface Species in Flotation Concentrates and Tails from ToF-SIMS Evidence, *Minerals Eng.*, Vol. 13, No. 13, 1377-1394.

## References

---

32. Poleunis, C., Rubio, C., Compère, C., and Bertrand, P., **2003**, ToF-SIMS Chemical Mapping Study of Protein Adsorption onto Stainless Steel Surfaces Immersed in Saline Aqueous Solutions, *Applied Surf. Sci.*, Vol. 203-204, 693-697.
33. Chryssoulis, S., Stowe, K., Niehus, E., Cramer, H.G., Bendel, C., and Kim, J., **1995**, Detection of Collectors on Mineral Grains by ToF-SIMS, *Trans. Inst. Min. Met.*, Vol 8, Section C, 141-150.
34. Karen, A., Man, N., Shibamori, T., and Takahashi, K., **2003**, ToF-SIMS Characterization of Industrial Materials: From Silicon Wafer to Polymer, *Applied Surf. Sci.*, Vol. 203-204, 541-546.
35. Rüdener, F.G., Riedel, M., Adams, F., Beske, H.E., Borodina, O., Düsterhöft, H., Gericke, M., Gijbels, R., Holzbrecher, H., Lodding, A., Lotockii, A., Mai, H., Michiels, F., Oswald, S., Richter, C.-E., Söderwall, G., Sólyom, A., Stahlberg, R., Steiger, W., Trapp, M., Stinger, G., and Voigtmann, R., **1990**, International Round-Robin Experiment for SIMS Quantification, *Periodica Polytech., Chem. Eng.*, Vol. 34, Nos. 1-3, 73-80.
36. Martin, C.J., Al., T.A., Cabri, L.J., **1997**, Surface Analysis of Particles in Mine Tailings by Time-of-Flight Laser-Ionization Mass Spectrometry (ToF-LIMS), *Environ. Geology*, Vol. 32, No. 2, 107-113.
37. Dimov, S.S. and Chryssoulis, S.L., **1998**, Standardization of Time-of-Flight Laser Ionization Mass Spectrometry Analysis of Minerals, *Spectrochim. Acta B*, Vol. 53, 399-406.
38. Shi, Y.J., Hu, X.K., Mao, D.M., Dimov, S.S., and Lipson, R.H., **1998**, Analysis of Xanthate Derivatives by Vacuum Ultraviolet Laser-Time-of-Flight Mass Spectrometry, *Anal. Chem.*, Vol. 70, 4534-4539.
39. Marabini, A. and Cozza, C., **1988**, A New Technique for Determining Mineral – Reagent Chemical Interaction Products by Transmission IR Spectroscopy: Cerussite – Xanthate System, *Colloids and Surfaces*, Vol. 33, 35-41.
40. Miettinen, M., Stén, P., Bäckman, S., Leppinen, J., and Aaltonen, J., **2000**, Determination of Chemicals Bound to Mineral Surfaces in Flotation Processes, *Minerals Eng.*, Vol. 13, No. 3, 245-254.
41. Termes, S. C. and Richardson, P. E., Application of FT-IR Spectroscopy for In Situ Studies of Sphalerite with Aqueous Solutions of Potassium Ethylxanthate and with Diethyldixanthogen, **1986**, *Int. J. Miner. Process.*, Vol. 18, 167-178.



## References

---

42. Baulsir, C. F. and Tague, T. J. Jr., **1998**, Introduction to Diffuse Reflectance Infrared Fourier Transform Spectroscopy, Spectra-Tech technical note, T2.
43. Persson, I., Persson, P., Valli, M., Fözö, S., and Malmensten, B. **1991**, Reactions on Sulfide Mineral Surfaces in Connection with Xanthate Flotation Studied by Diffuse Reflectance FTIR Spectroscopy, Atomic Absorption Spectrophotometry and Calorimetry, *Int. J. Miner. Process.*, Vol. 33, 67-81.
44. Contini, G., Ciccioli, A., Cozza, C., Barbaro, M., and Marabini, A.M., **1997**, Infrared Study of 2-mercaptobenzothiazole and Two of its Derivatives Adsorbed on PbS, *Int. J. Miner. Process.*, Vol. 51, 283-291.
45. Leppinen, J. O., Basilio, C. I., and Yoon, R. H. **1989**, In-Situ FTIR Study of Ethyl Xanthate Adsorption on Sulfide Minerals under Conditions of Controlled Potential, *Int. J. Miner. Process.*, Vol. 26, 259-274.
46. Cases, J. M. and De Donato, P. **1991**, FTIR Analysis of Sulphide Mineral Surfaces Before and After Collection: Galena, *Int. J. Miner. Process.*, Vol. 33, 49-65.
47. Leppinen, J. O. **1990**, FTIR and Flotation Investigation of the Adsorption of Ethyl Xanthate on Activated and Non-activated Sulfide Minerals, *Int. J. Miner. Process.*, Vol. 30, 245-263.
48. Popov, S. R. and Vučinić, D. R. **1990**, The Ethylxanthate Adsorption on Copper-activated Sphalerite under Flotation-related Conditions in Alkaline Media, *Int. J. Miner. Process.*, Vol. 30, 229-244.
49. Ihs, A. and Liedberg, B. **1994**, Infrared Study of Ethyl and Octyl Xanthate Ions Adsorbed on Metallic and Sulfidized Copper and Silver Surfaces, *Langmuir*, Vol. 10, 734-740.
50. Larsson, M. L., Holmgren, A., and Forsling, W. **2000**, Xanthate Adsorbed on ZnS Studied by Polarized FTIR-ATR Spectroscopy, *Langmuir*, Vol. 16, 8129-8133.
51. Singh, P. K., Adler, J. J., Rabinovich, Y. I., and Mougdil, B. M. **2001**, Investigation of Self-Assembled Surfactant Structures at the Solid-Liquid Interface Using FT-IR/ATR, *Langmuir*, Vol. 17, 468-473.
52. Kariis, H., <http://www.ifm.liu.se/~hanka/methods/raman.shtml>, March 12<sup>th</sup>, **1998**.
53. Woods, R., Hope, G. A., and Watling, K., **2000**, Surface Enhanced Raman Scattering Spectroscopic Studies of the Adsorption of Flotation Collectors, *Minerals Eng.*, Vol. 13, No. 4, 345-356.

## References

---

54. Woods, R., Hope, G.A., and Watling, K., **2000**, A SERS Spectro-electrochemical Investigation of the Interaction of 2-Mercaptobenzothiazole with Copper, Silver and Gold Surfaces, *J. Applied Electrochem.*, Vol. 30, 1209-1222.
55. Hope, G.A., Woods, R., and Watling, K., **2003**, A Spectroelectrochemical Investigation of the Interaction of Diisobutyldithiophosphinate with Copper, Silver and Gold Surfaces: II. Electrochemistry and Raman Spectroscopy, *Colloids and Surfaces A: Physicochem. Eng. Aspects*, Vol. 214, 87-97.
56. Prestidge, C. A., Thiel, A. G., Ralston, J., and Smart, R. St. C., **1994**, The interaction of ethyl xanthate with copper(II)-activated zinc sulphide: kinetic effects, *Colloids and Surfaces A: Physicochem. Eng. Aspects*, Vol. 85, 51-68.
57. Haines, P.J., **1995**, "Thermal Methods of Analysis: Principles, Applications and Problems", Blackie Academic & Professional, Chapman & Hall, Glasgow, 286p.
58. Howe, T.M. and Pope, M.I., **1970-71**, The Quantitative Determination of Flotation Agents Adsorbed on Mineral Powders, Using Differential Thermal Analysis, *Powder Tech.*, Vol. 4, 338-344.
59. Vreugdenhil, A. J., Brienne, S. H. R., Butler, I. S., Finch, J. A., and Markwell, R. D., **1997**, Infrared Spectroscopic Determination of the Gas-phase Thermal Decomposition Products of Metal-ethyldithiocarbonate Complexes, *Spectrochim. Acta A*, Vol. 53, 2139-2151.
60. Dunn, J.G., Chamberlain, A.C., Fisher, N.G., and Avraamides, J., **1997**, The Influence of Activated Carbon on the Thermal Decomposition of Sodium Ethyl Xanthate, *J. Thermal Analysis*, Vol. 49, 1399-1408.
61. Fisher, N.G. and Dunn, J.G., **2000**, Identifying Organic Foulants on Activated Carbon from Gold Processing Plants, *Minerals Eng.*, Vol. 13, No. 14-15, 1581-1588.
62. Dunn, J.G. and Fisher, N.G., **2001**, Thermal Decomposition of Frothing Agents Adsorbed onto Activated Carbon, *Thermochim. Acta*, Vol. 366, 157-166.
63. Fisher, N.G. and Dunn, J.G., **1999**, Analysis of a Complex Gaseous Mixture by TG-MS and TG-FTIR, *J. Thermal Analysis and Calorimetry*, Vol. 56, 43-49.
64. Jackson, R.S. and Rager, A., **2001**, The Use of Reduced Pressure to Expand the Capabilities of TGA-FTIR, *Thermochim. Acta*, Vol. 367-368, 415-424.

## References

---

65. Vreugdenhil, A. J., Brienne, S. H. R., Markwell, R. D., Butler, I. S., and Finch, J. A. **1997**, Headspace Analysis Gas-Phase Infrared Spectroscopy: a Study of Xanthate Decomposition on Mineral Surfaces, *J. Mol. Struct.*, Vol. 405, 67-77.
66. Vreugdenhil, A. J., Finch, J. A., Butler, I. S., and Paquin, I. **1999**, Analysis of Alkylxanthate Collectors on Sulphide Minerals and Flotation Products by Headspace Analysis Gas-Phase Infrared Spectroscopy (HAGIS), *Minerals Eng.*, Vol. 12, No. 7, 745-756.
67. Lascelles, D., Finch, J. A., and Butler, I. S., **2001**, Headspace Analysis Gas-Phase Infrared Spectroscopy: Investigating the Thermal Decomposition Products of Mineral Flotation Collectors, 11<sup>th</sup> annual Can. Thermal Analysis Soc. Tech. Meeting, Ottawa, May 15-16.
68. Leja, J., **1982**, "Surface Chemistry of Froth Flotation", Plenum Publishing Corporation, Ch. 5.
69. Vreugdenhil, A.J., **1996**, "Applications of Vibrational Spectroscopy to Inorganic Environmental and Industrial Systems", Ph.D. thesis, McGill University.
70. Ralston, J., **1994**, The Chemistry of Galena Flotation: Principles and Practice, *Minerals Eng.*, Vol. 7, Nos 5/6 pp. 715-735.
71. Naklicki, M.L., Rao, S.R., Gomez, M., and Finch, J.A., **2002**, Flotation and Surface Analysis of the Nickel(II) Oxide / Amyl Xanthate System, *Int. J. Miner. Process.*, Vol. 65, pp. 73-82.
72. Lascelles, D. and Finch, J.A., **2004**, Quantification of Adsorbed Reagents: Xanthates, submitted to *Minerals Eng.*
73. Sproule, K., Harcourt, G.A., and Rose, E.H., **1945**, Froth Flotation of Nickel-Copper Matte, U.S. Patent, No. 2,432,456.
74. Xu, Z., Rao, S.R., Finch, J.A., Kelebek, S. and Wells, P., **1997**, Role of Diethylenetriamine (DETA) in Pentlandite-Pyrrhotite Separation – Part 1: Complexation of Metals with DETA, *Trans. IMM*, Section C, Vol. 106, pp. C15-C20.
75. Yoon, R.-H., Basilio, C.I., Marticorena, M.A., Kerr, A.N. and Stratton-Crawley, R., **1995**, A Study of the Pyrrhotite Depression Mechanism by Diethylenetriamine, *Minerals Eng.*, Vol. 8, No. 7, pp. 807-816.

## References

---

76. Robertson, G., Internal communication, Inco Technical Services Ltd., Project #55-131.
77. Welti, D., **1970**, Infrared Vapour Spectra, Heyden and Son Ltd., New York, NY, USA.